Author Manuscript

Author Manuscript

Author Manuscript

Author Manuscript

HHS Public Access

Author manuscript

Virology. Author manuscript; available in PMC 2019 March 01.

Published in final edited form as:

Virology. 2018 September ; 522: 244–259. doi:10.1016/j.virol.2018.06.018.

Chikungunya-vesicular stomatitis chimeric virus targets and eliminates brain tumors

Xue Zhang[1], **Guochao Mao**[1], and **Anthony N. van den Pol**[*]

Department of Neurosurgery, Yale University School of Medicine, 333 Cedar St, New Haven, CT 06520, United States

Abstract

Vesicular stomatitis virus (VSV) shows potential for targeting and killing cancer cells, but can be dangerous in the brain due to its neurotropic glycoprotein. Here we test a chimeric virus in which the VSV glycoprotein is replaced with the Chikungunya polyprotein E3-E2-6K-E1 (VSVΔG-CHIKV). Control mice with brain tumors survived a mean of 40 days after tumor implant. VSVΔG-CHIKV selectively infected and eliminated the tumor, and extended survival substantially in all tumor-bearing mice to over 100 days. VSVΔG-CHIKV also targeted intracranial primary patient derived melanoma xenografts. Virus injected into one melanoma spread to other melanomas within the same brain with little detectable infection of normal cells. Intravenous VSVΔG-CHIKV infected tumor cells but not normal tissue. In immunocompetent mice, VSVΔG-CHIKV selectively infected mouse melanoma cells within the brain. These data suggest VSVΔG-CHIKV can target and destroy brain tumors in multiple animal models without the neurotropism associated with the wild type VSV glycoprotein.

Keywords

Oncolytic; VSV; Brain; Glioma; Melanoma; Chikungunya; Neuron; Chimeric virus

1. Introduction

Vesicular stomatitis virus (VSV) is an enveloped, negative-sense, single-strand RNA virus in the *Rhabdoviridae* family. While rarely causing disease in humans, the virus can pose a potential threat to livestock including cattle, horses, and pigs (Lyles and Rupprecht, 2007). In recent years, recombinant altered versions of VSV have shown considerable potential as the molecular basis for live vaccines engineered to express antigenic proteins from other viruses (Kurup et al., 2015; Clarke et al., 2006; Geisbert et al., 2008, 2009). VSV has also shown promise as an oncolytic virus (Wongthida et al., 2011; Obuchi et al., 2003; Ozduman et al., 2008; van den Pol and Davis, 2013; Wollmann et al., 2005). However, a substantive limitation of VSV is that the VSV glycoprotein is highly neurotropic, and upon entering the brain, can lead to deleterious neurological consequences, including death (Huneycutt et al., 1993; Lundh et al., 1987, 1988; van den Pol et al., 2002).

[*]Corresponding author. anthony.vandenpol@yale.edu (A.N. van den Pol).

[1]These authors contributed equally and are considered joint first authors.

Author Manuscript Author Manuscript Author Manuscript Author Manuscript

Although substitution of glycoprotein genes from other viruses can reduce VSV neurotropism (Wollmann et al., 2015; van den Pol et al., 2017a), the attenuation of neurotropism is not necessarily a universal attribute of chimeric VSVs. Glycoproteins from some viruses that have been substituted for the VSV glycoprotein can be maladaptive and enhance neurotropism; for example the replication competent Nipah-VSV chimera is lethal in the brain (van den Pol et al., 2017a). Even for the potential treatment of non-brain cancers with oncolytic viruses, the importance of attenuating or eliminating the neurotropism of VSV is suggested by data showing that metastatic myeloma cancer cells can form a bridge from outside the brain across the meninges into the brain, potentially serving as a conduit through the blood brain barrier for a neurotropic virus to enter the brain (Yarde et al., 2013).

Chikungunya virus (CHIKV) is a positive-sense single-strand RNA virus of the alphavirus genus and Togavirus family. Prior to 2013 it was primarily found in Asia, Africa, and Europe; starting in 2013 the virus has been spread by mosquitoes through most of South America and parts of North America with primates as a potential reservoir (https://www.cdc.gov/chikungunya/geo/index.html; Vignuzzi and Higgs, 2017; Vu et al., 2017). There is currently no approved vaccine available; a number of different experimental vaccines are being tested (Chattopadhyay et al., 2013; Powers, 2018; Yang et al., 2017). CHIKV has generally been associated with fever and joint pain, but can also cause headache, muscle ache, and rash (Hua and Combe, 2017; Amdekar et al., 2017). The joint pain can persist for many months or longer. Chikungunya may bind to one of several surface proteins which have been suggested to include cholesterol transporters, prohibitin and others (Wichit et al., 2017; Wintachai et al., 2012) and appears to be internalized in clathrin coated pits (Bernard et al., 2010; Schwartz and Albert, 2010; Hoornweg et al., 2016). VSV has been proposed to utilize the LDL receptor as an entry port (Finkelshtein et al., 2013).

Here we test a CHIKV-VSV chimeric virus containing a portion of the CHIKV structural polyprotein that includes the E3-E2-6K-E1 glycoprotein sequence substituted for the VSV glycoprotein (Chattopadhyay et al., 2013). CHIKV E2 underlies receptor binding, and E1 is responsible for the low pH membrane fusion activity after endocytotic entry (Voss et al., 2010; Solignat et al., 2009). Together E2 and E1 constitute spike-like trimers on the virus surface. E3 is postulated to prevent premature virus fusion (Uchime et al., 2013), and 6K enhances virion release and titer (Taylor et al., 2016). VSV in which the normal glycoprotein gene G has been deleted and replaced by genes coding for the CHIKV envelope glycoprotein (VSVΔG-CHIKV) appears safe within the brain and, as tested in rodents, did not evoke neurological dysfunction or substantive negative consequences (van den Pol et al., 2017a).

Here we address the question of whether this VSVΔG-CHIKV chimera can selectively infect and cytolytically kill brain tumor cells without substantive damage to normal cells in the brain.

Author Manuscript Author Manuscript Author Manuscript Author Manuscript

2. Results

2.1. Human cancer cells have high susceptibility to CHIKV

A CHIKV-VSV chimera VSVΔG-CHIKV was used in which the VSV glycoprotein was replaced with the glycoprotein sequence from CHIKV (Fig. 1A). To determine whether VSVΔG-CHIKV displayed a preferential infection of cancer cells, we compared a variety of different cell types including both cancer and non-cancer normal control cells. The cells used included human glioma U373, U118 and U87 and the mouse glioma CT-2A, along with normal human glia and normal mouse glia. Additional cancer types included the human melanoma cells YUMAC and 501mel, and the breast cancer cells MDA-MB-436, MDA-MB-231 and BT-549. Cells were inoculated using an MOI of 0.02 and VSVΔG-CHIKV infection was determined by immunostaining at 3 days post-infection (dpi). The percentage of infected human glioma cells (n = 6 samples/group) was substantially greater than that of normal human glia (U373 $p < 0.001$; U118 $p < 0.01$; U87 $p < 0.01$; ANOVA) (Fig. 1B,D). Additionally, the percentage of infected human melanoma and breast cancer cells was also significantly greater than control normal human cells (glia) (ANOVA) (Fig. 1C and D). Mouse glioma CT-2A cells also showed a greater percentage of infected cells than normal mouse glia, but displayed less infection than human gliomas (Fig. 1B,D).

To compare relative levels of infection and replication of VSVΔG-CHIKV in different cell types, we compared virus plaque size on glioma, melanoma, breast cancer and normal human brain cells at 3 days (Fig. 2A). All human glioma cell lines yielded large plaques (n = 20 plaques/group $p < 0.001$ vs normal human glia, ANOVA), whereas on normal human glia VSVΔG-CHIKV displayed significantly smaller plaques (Fig. 2B,D). Both mouse glioma (CT-2A) and normal mouse glia appeared less susceptible to VSVΔG-CHIKV. In comparisons of breast cancer cells, BT-549 displayed a significantly larger (n = 20 plaques; $p < 0.001$; ANOVA) plaque size than MDA-MB-231 or MDA-MB-436 cells. YUMAC and 501 human melanoma cells also yielded larger plaques than normal human cells (Fig. 2C,D). Infected cells ultimately showed a lethal response to virus infection as corroborated with ethidium homodimer labeling.

2.2. VSVΔG-CHIKV selectively infects a broad range of human glioma

In order to examine further the susceptibility of human glioma cells to VSVΔG-CHIKV infection, a panel of different glioma with different growth characteristics and mutational defects were infected with VSVΔG-CHIKV at a low MOI of 0.02. 24 h later, VSVΔG-CHIKV not only infected the inoculated cells (Fig. 3A, left) but additionally showed significant replication (Fig. 3A, right) after secondary inoculation (24 h) of fresh cultures with media collected from infected cultures, as suggested above in the plaque analysis. In contrast to the human glioma cells, normal human astrocytes showed attenuated infection and little evidence of virus replication. Similarly, normal mouse glia supported little infection or replication of VSVΔG-CHIKV whereas mouse CT-2A glioma cells displayed both infection and replication (Fig. 3B,D).

Author Manuscript Author Manuscript Author Manuscript Author Manuscript

2.3. Comparison of recombinant VSV infection of glioblastoma

To determine the susceptibility of glioma cells to VSVΔG-CHIKV infection, two additional recombinant VSVs, one wild-type (VSVwt) and another chimeric VSV, VSV-LASV-GPC (VSVΔG-LASV) were compared with VSVΔG-CHIKV for their ability to infect and kill either mouse (CT-2A) or human (U118) derived glioma cells (Fig. 4A–D). Twenty-four hours after inoculation (MOI =1) all three viruses showed good infection levels at 24 hpi (Fig. 4A,B) and evoked cell death at 48 hpi as determined with ethidium homodimer (Fig. 4C,D) in both mouse and human glioma cells. VSVwt showed greater infection and cell death than VSVΔG-CHIKV or VSVΔG-LASV. Non-infected control tumor cells showed no infection and little cell death.

To compare the relative propagation of these 3 viruses, viral plaque size was measured using monolayer cultures of human (U118, U87) and mouse (CT-2A) glioma (Fig. 4E, F). Forty-eight hours after infection both human glioma cell lines yielded robust large plaques; mouse CT-2A yielded smaller plaques for all 3 viruses. As expected the VSVwt plaques were larger than those generated by VSVΔG-CHIKV or VSV LASV-GPC.

2.4. Type I interferon actions on VSVΔG-CHIKV infection of human glioma

Interferons (IFNs) are cytokines that play a critical role in the induction and maintenance of innate and adaptive immunity, and dys-functional IFN signaling has been suggested as a key mechanism contributing to enhanced infection of cancer cells (Stojdl et al., 2000). To test whether type I interferon might play a role in the selectivity of VSVΔG-CHIKV infection of cancer cells, glioma cells and normal cells were cultured and pre-treated with 1 or 10 IU of a recombinant hybrid type I interferon (IFN-αA/D that activates both mouse and human type 1 IFN receptors) for 12 h prior to infection with VSVΔG-CHIKV at an MOI of 0.02 (Fig. 5). Twenty-four hours later, immunostaining was used to quantify the number of cells showing VSVΔG-CHIKV infection. IFN-α (1 IU, n = 6 samples/group) almost completely blocked VSVΔG-CHIKV infection of normal astrocytes compared to no IFN ($p < 0.01$ vs. control) (Fig. 5A,C). In contrast to IFN's block of infection in normal human astrocytes, viral infection of human glioma U118, U87, and U373 was attenuated but not completely blocked by IFN-α at 1 IU (U118, $p = 0.37$; U87, $p = 0.37$; U373, $p = 0.058$; vs no-IFN controls). As expected, a greater effect was observed at 10 IU in a dose-dependent manner ($p < 0.001$ vs control) (Fig. 5A,C). VSVΔG-CHIKV showed only modest inhibition by IFN-α in mouse CT-2A glioma (Fig. 5B,D).

2.5. VSVΔG-CHIKV targets glioma

To examine whether VSVΔG-CHIKV can act in vivo, the mouse brain was injected with glioblastoma rU118, and rU373 cells. Nine days after tumor injection into the striatum of SCID mice, VSVΔG-CHIKV (7×10^8 PFU) was injected intracranially in the area of the tumor. Mice were euthanized 4, 7, and 15 days later (Fig. 6A). Four days after VSVΔG-CHIKV administration (13 days after injection of cancer cells), the virus showed selective infection of all types of glioma including U118 (n = 3) (Fig. 6B–F) and U373 (n = 4) (not shown). At 7 and 15 dpi, a greater number of tumor cells were selectively infected (Fig. 6B–F). In contrast to the infection of glioma (Fig. 6B–F), little infection was detected in the normal host brain.

Author Manuscript Author Manuscript Author Manuscript Author Manuscript

2.6. VSVΔG-CHIKV enhances survival in brain tumor bearing mice

In the experiments above, we show that VSVΔG-CHIKV selectively targets gliomas in vitro and in vivo. Here we address the hypothesis that VSVΔG-CHIKV will improve the survival of tumor-bearing mice. Human U87 glioma were implanted into the brains of SCID mice (n = 22). After the tumors had expanded for 8 days, VSVΔG-CHIKV was injected into the tumor (n = 10); other mice (n = 10) served as tumor bearing controls with no virus. As a positive control, we also used VSV-LASV-GPC (n = 2) which had been previously shown to enhance survival in tumor-bearing mice (Wollmann et al., 2015).

VSVΔG-CHIKV greatly enhanced the survival of tumor-bearing mice. All tumor-bearing mice (n = 10) not treated with virus showed a lethal response to the expanding tumor with a mean survival of 38 days post-tumor implantation, and a maximum survival of 44 days post-tumor implantation (Fig. 7). A photomicrograph of an untreated brain shows substantial tumor expansion and encroachment into the adjacent normal brain (Fig. 8A). In striking contrast, all tumor-bearing mice (n = 10) treated intracranially with VSVΔG-CHIKV showed a statistically significant extended long-term survival of 100 days post-tumor implantation (Fig. 7) ($p < 0.001$; log-rank test). At that point, one or two mice were euthanized by anesthetic overdose every few days up to 120 days. None of the tumor-bearing mice treated with VSVΔG-CHIKV showed a lethal response either to tumor-mediated brain dysfunction or to the presence of VSVΔG-CHIKV within the brain. Histological verification in the brains of tumor-bearing mice treated with VSVΔG-CHIKV show an apparent absence of tumor, and an absence of detectable virus in an additional mouse euthanized 108 days after tumor implant and treated with intratumoral VSVΔG-CHIKV (Fig. 8D–E). The tumor-bearing mice (n = 2) treated with the positive control VSV-LASV-GPC also showed extended survival (Figs. 7, 8C, 9C,D) as previously reported (Wollmann et al., 2015). Fig. 9A shows large red tumors in the brains of 5 mice that did not receive VSVΔG-CHIKV, and the absence of detectable tumor in the brains of 5 other mice that did receive VSVΔG-CHIKV (Fig. 9B).

2.7. VSVΔG-CHIKV infects human melanoma

In the paragraphs above, we focus on the potential of VSVΔG-CHIKV to infect glioma within the brain. Here we test the hypothesis that VSVΔG-CHIKV can selectively infect other types of brain cancer cells. Nine days after injection and expansion of primary human rYUMAC melanoma into the SCID mouse brain, VSVΔG-CHIKV was injected into the brain (n = 3) (Fig. 10A). Strong green viral immunofluorescence was found in the tumors with little infection outside the melanoma cells at the different time points examined. At 4 dpi many, but not all, tumor cells showed infection (Fig. 10B). At 7 dpi (Fig. 10C) and 15dpi (Fig. 10D), the percentage of infected cells increased, and the cells showed additional signs of viral infection.

2.8. VSVΔG-CHIKV migrates to multiple tumors in a model of metastatic brain cancer

The current standard clinical treatment of brain tumors is surgical resection of the malignant tissue, combined with radiotherapy and chemotherapy (Wei et al., 2015; Wollmann et al., 2012). However, in patients with high grade brain tumors, neurosurgical removal or focused

Author Manuscript Author Manuscript Author Manuscript Author Manuscript

radiation may eliminate the main tumor body but is generally unable to eliminate the large number of tumor cells that have migrated into the surrounding brain tissue.

To evaluate the efficacy and safety of selective tumor reduction by VSVΔG-CHIKV and its impact on melanoma, we implanted the left and right side of the SCID mouse brain with human primary rYUMAC melanoma (in striatum or cortex) (Fig. 11A). 8 days later, VSVΔG-CHIKV was stereotactically injected unilaterally only into the tumor on the right side of the brain. Eight days later, the animals were euthanized and the brains were examined. VSVΔG-CHIKV completely destroyed the inoculated tumor on the right side of the brain (Fig. 11B and D). Additionally, the virus migrated to the contralateral left tumor (striatum and cortex) and began the process of infection and destruction without infecting the intervening normal brain (Fig. 11C and E). These results suggest that VSVΔG-CHIKV can selectively infect multiple brain tumors after injection into a single tumor.

To further confirm VSVΔG-CHIKV selectively infected melanoma in vivo, we implanted both sides of the SCID mouse brain (n = 3) with human primary rYUMAC melanoma cells (in striatum). 10 days later, VSVΔG-CHIKV was stereotactically injected into the dorsal region of the tumors on both sides of the brain. Two days later the tumors, along with control samples of cerebellum, were harvested, dissociated, and used to inoculate Vero cells. Nearly all of the Vero cells were infected by the extracted tumor tissue (99.1% ± 0.6), whereas none of the cultured cells receiving normal cerebellar tissue from the same brain became infected (Fig. 11F–H). In additional experiments conducted at 10 dpi, we found a similarly robust infection of Vero cells (77.5% ± 3.0) after inoculation with dissociated tumor samples and no detectable infection conferred by normal cerebellar tissue.

2.9. Mouse melanoma in immunocompetent mouse brain

To test the ability of VSVΔG-CHIKV to target tumor cells in an immunocompetent animal model, B16 mouse melanoma cells were tested. VSVΔG-CHIKV showed strong infection of cultured mouse melanocytes (Fig. 12A,B) and generated large plaques indicating infection, replication, and release. B16 melanoma cells were injected into the brains of normal C57/Bl6 mice (n = 3). Seven days later after the tumor cells had expanded, VSVΔG-CHIKV (2.25×10^5 PFU in 0.75 μl) was injected directly into the brain in the area of the tumor. Three and four days later, brains were harvested. The mouse melanoma cells could be distinguished from the host brain by the dark coloration of the melanosomes within the mouse melanoma in contrast to the absence of such a dark coloration in the host brain cells. Green virus immunofluorescence was found primarily in the mouse melanoma cells, with the virus immunofluorescence overlapping with the dark- colored melanoma cells (Fig. 12D,E).

2.10. Intravenous VSVΔG-CHIKV selectively infects subcutaneous melanoma

To study the potential of the virus to infect distant tumors, eleven days after subcutaneous implant of rYUMAC human melanoma, VSVΔG-CHIKV was injected into the tail vein, and 4 days later mice (n = 5) were euthanized. VSVΔG-CHIKV was found only in the melanoma, (Fig. 13A–C). We also asked whether the virus would infect other tissue in these immunodeficient SCID mice. We found no VSVΔG-CHIKV immunoreactivity in lung,

Author Manuscript Author Manuscript Author Manuscript Author Manuscript

colon, bladder, kidney, heart, stomach, testis, brain, liver (Fig. 13D), or spleen. These data suggest that the virus shows considerable selectivity to tumors and not to any of the other organs studied.

3. Discussion

Here we show that a chimeric virus, VSVΔG-CHIKV, consisting of 4 genes (N,P,M,L) from VSV, and genes coding for the CHIKV glycoprotein sequence (E3-E2-6K-E1) substituted for the VSV glycoprotein gene (G) in the 4th genomic position of VSV results in an oncolytic virus that can safely and selectively target, infect, replicate in, and destroy both glioma and melanoma within the brain. The substitution of the CHIKV glycoprotein for the VSV glycoprotein improves safety in the brain dramatically. Whereas the native VSV glycoprotein is strongly neuro-tropic and can lead to a lethal response in the brain, the elimination of the VSV G and substitution of the CHIKV glycoprotein not only improves safety in the brain (van den Pol et al., 2017a), but results in a chimeric virus that can selectively target tumors within the brain and dramatically improve survival of brain-tumor bearing mice.

Although wild-type VSVs and VSVs with modest genetic mutations that attenuate the virus can target a number of different cancer cells (Wollmann et al., 2005) by several mechanisms (Cary et al., 2011), a key limitation of VSV is the neurotropism of the virus with the normal viral glycoprotein which can lead to adverse consequences including a lethal response (Huneycutt et al., 1993; Lundh et al., 1987, 1988; van den Pol et al., 2002). Although CNS complications of VSV can be attenuated by peripheral vaccination (Ozduman et al., 2009), various antiviral drugs or strong type 1 interferon expression (Wollmann et al., 2015), avoiding a neurotropic phenotype may constitute a safer and better approach, as we demonstrate here. Importantly, VSVΔG-CHIKV is not only safe in the brains of normal mice, it is also safe in the brains of immunocompromised SCID mice with little T and B cell systemic immunity, as we show here, suggesting that the innate immune system within the brain has the potential to block virus replication in normal neurons and glial cells.

Attenuated VSVs retaining the VSV glycoprotein demonstrate the potential to target cancer cells, including glioma outside the brain (Lun et al., 2006; Cary et al., 2011) and inside the brain (Ozduman et al., 2008). A VSV expressing beta-interferon is being used in clinical tests against liver cancer and has shown an very good safety profile outside the brain (Zhang et al., 2016a, 2016b; Naik et al., 2015), but can still be problematic inside the brain (Wollmann et al., 2015). VSV targeting tumors within the brain may show attenuated neuropathic actions due to possible upregulation of innate immunity in the brain due to the presence of nearby foreign cells (the surgically implanted tumor) and by potential low level IFN signaling from the infected tumor to surrounding brain. Interferon stimulated genes may be upregulated even by distant interferon signaling within the brain (van den Pol et al., 2014).

Although here we focus mostly on one resident type of brain tumor, gliomas, and one metastatic brain tumor, melanoma, VSVΔG-CHIKV also infects a number of other types of cancer cell. In addition to gliomas and melanomas, we also show infection of breast cancer

Author Manuscript Author Manuscript Author Manuscript Author Manuscript

in vitro. We find that VSVΔG-CHIKV selectively targets a type of cancer cell that originates from melanocytes in the skin and metastasizes into the brain. For these experiments we employed primary patient derived melanoma xenografts after minimal expansion in vitro. We show with four different animal models that VSVΔG-CHIKV selectively targets tumors. These models include glioma cell line experiments, patient derived (melanoma) xenografts (PDX) with direct intratumoral injection and with intravascular injection leading to selective tumor infection, and mouse tumors in immunocompetent mice. Although cancer cell lines can accumulate mutations over extended periods in culture, the PDX cells had minimal time in culture, suggesting that VSVΔG-CHIKV targeting to tumor cells was not dependent on excessive culture-evoked mutational accumulations.

In addition to select infection of tumor cells within the brain, VSVΔG-CHIKV has the potential to target and selectively infect cells that have migrated away from the main tumor body. In a model of brain metastasis, multiple melanoma tumor sites were initiated within the brain. Subsequent to selective infection of one tumor (melanoma), the virus migrated away from the injected tumor to selectively infect another experimental tumor within the same brain. This was true both when the secondary tumor was situated in the mirror contralateral striatum, and also when the secondary tumor was situated in the contralateral cerebral cortex and the primary tumor was in the striatum. Infection of multiple tumors in a single brain was accomplished with little detectable infection in the normal brain between the two tumors.

We previously showed that a chimeric virus consisting of VSV and the Ebola glycoprotein substituted for the VSV glycoprotein could also target brain tumors, but importantly, the VSV-EBOV-GP did not completely eliminate the tumors, as shown both by histological verification of incomplete tumor infection, as well as the generation of only a modest improvement in survival of mice with brain tumors when treated with VSV-EBOV-GP (Wollmann et al., 2015). The modest anti-brain tumor response of VSV-EBOV-GP contrasts with the much more robust VSVΔG-CHIKV data here showing complete elimination of brain tumors and substantial (complete) increase in survival, at least for the duration of the survival experiments of several months. The mechanism behind this difference is not clear, but may relate to some enhanced innate or systemic immune block of the VSV-EBOV-GP compared with VSVΔG-CHIKV; although the SCID mice used in these experiments are attenuated in T- and B- cell and other adaptive immune responses, they still retain innate immune potential and may show some reduced adaptive immune responses.

The success of VSVΔG-CHIKV in destroying brain tumors raises the question of whether it might have clinical potential. Recombinant VSVs are currently being tested in humans. The chimeric VSV-EBOV-GP has shown substantial potential as a vaccine in central Africa against Ebola virus (Banadyga and Marzi, 2017) and with greater anti-Ebola efficacy than other vaccine platforms; the results in humans were consistent with earlier data showing substantial anti-Ebola efficacy in non-human primates (Geisbert et al., 2008, 2009; Marzi et al., 2015, 2016). In addition, the VSV-EBOV-GP was found to be safe when injected into the non-human primate brain (Mire et al., 2012). A recombinant VSV with the native VSV glycoprotein that expresses a type 1 interferon is also being tested in human clinical trials for liver cancer (Zhang et al., 2016a, 2016b).

Author Manuscript Author Manuscript Author Manuscript Author Manuscript

Other viruses, for instance some strains of measles virus (Allen et al., 2008, 2013) may be able to safely target brain tumors, and in conjunction with immunomodulators, show promise in the brain (Hardcastle et al., 2017). In addition to its direct oncolytic action (Wollmann et al., 2005; Cary et al., 2011), VSV is also immunogenic, and can enhance an immune attack on cancer cells that have been infected, generalizing to other similar non-infected cancer cells (Galivo et al., 2010).

In addition to the CHIKV glycoprotein sequence, two other VSVs with different glycoproteins used in place of VSV G have been described, including lymphocytic choriomeningitis virus glycoprotein (Muik et al., 2011) and Lassa fever virus glycoprotein (Wollmann et al., 2015). This raises the question of whether the use of multiple chimeric VSVs may have some benefit. In successive uses of an experimental VSV vaccine with the same VSV glycoprotein, on repeated immunizations the immune system targeted the VSV glycoprotein rather than the accompanying HIV antigen of interest, thereby defeating the potential for vaccination against AIDS. However, the use of three different VSV glycoproteins in successive vaccinations enhanced the immune response to the HIV protein of vaccine interest (Rose et al., 2001). This points at the possible advantage of potentially employing different glycoproteins if more than one treatment with an oncolytic virus may be needed to generate a directed immune response against an infectible tumor.

Despite improved safety for these chimeric viruses, one cannot assume safety simply by substitution of alternate viral glycoproteins. In contrast to the improved safety within the brain of the viruses above, substitution of the influenza glycoprotein for VSV G retained neurotropism in early stages of brain development, or worse, substitution of Nipah virus F +G glycoproteins resulted in a recombinant virus that was even more lethal than wild-type VSV within the brain (van den Pol et al., 2017a). VSV that expressed only Nipah F or Nipah G was replication-restricted and as such was safe in the brain (van den Pol et al., 2017a) and retained a capacity for immunization against Nipah virus (Chattopadhyay et al., 2013).

In a minority of cases, particularly in neonates, infection with wild-type CHIKV has been linked to neurological complications including external facial palsy, Guillain-Barré syndrome, menigoencephalitis, myelitis, myeloneuropathy, optic neuritis, and sensorineural deafness (Chandak et al., 2009; Das et al., 2010; Pinheiro et al., 2016; Gasque, 2013). That association with neurological complications in the parent CHIKV virus may not lead to negative consequences in the related chimeric virus is suggested by findings with a chimeric virus where the neurotropic rabies virus glycoprotein gene was substituted for the VSV glycoprotein gene. Whereas rabies virus itself is lethal in the brain, the chimeric VSVΔG-RABV was not lethal and was substantially safer than either VSV or rabies virus in the brain (Beier et al., 2011, 2013). In animal models, some strains of CHIKV were found to evoke neurological infection and dysfunction in mouse brain, and similar to a number of other viruses was most problematic in the developing brain (Das et al., 2010; Ziegler et al., 2008; Powers and Logue, 2007; van den Pol et al., 2002, 2017a, 2017b). In contrast, the VSVΔG-CHIKV tested here did not show the same spread within the brain and did not appear to lead to negative consequences. Even in immunocompromised SCID mice, after intracranial injection VSVΔG-CHIKV showed little spread in the brain and no lethal actions.

Author Manuscript Author Manuscript Author Manuscript Author Manuscript

Together, these data suggest that VSVΔG-CHIKV merits further consideration as a virus that can safely target, infect, and kill both resident (glioma) and metastatic (melanoma) cancer cells within the brain in multiple animal models.

4. Materials and methods

4.1. Virus and cells

VSVΔG-CHIKV was generated by replacing the VSV G gene with the genes coding for the entire CHIKV envelope polyprotein (E3-E2-6K-E1) derived from the prototypic African strain CHIKV S27, as described previously (Chattopadhyay et al., 2013). This CHIKV-VSV chimera incorporated functional CHIKV glycoproteins into the viral envelope resulting in a replication competent virus. To demonstrate that this chimeric virus showed the proper incorporation of CHIKV glycoproteins, VSVΔG-CHIKV was tested with ^{35}S labeling of CHIKV envelope poly-protein and measurements of replication kinetics (one-step growth curves) comparing VSVΔG-CHIKV and the parental recombinant wild-type VSV (VSVwt) (Chattopadhyay et al., 2013). Stocks of VSVΔG-CHIKV were grown and harvested using BHK-21 cells and titers of harvested viral stocks were determined by plaque assay using Vero cells. VSV-LASV-GPC used in vivo is a VSV chimera with the Lassa fever virus glycoprotein gene replacing the VSV glycoprotein gene (gift of Drs. C.Cepko, S.Whelan, Harvard University, Boston, MA) (Wollmann et al., 2015; Jae et al., 2013). VSV-LASV-GPC used in vitro was kindly provided by Dr. H. Feldmann (NIH Rocky Mountain Laboratories, Hamilton, MT) (Wollmann et al., 2015; Garbutt et al., 2004). VSVwt is a recombinant wild-type VSV (from Dr. J.K. Rose, Yale Univeristy) (Lawson et al., 1995).

Human glioma U87 and U118 cells were obtained from ATCC (Manassas, VA). Mouse glioma CT-2A cells (gift of Dr.T.Seyfried; Boston College). We complement widely used cell lines where cell identity can become uncertain with recent local patient-derived tumor samples. YUMAC and 501mel human melanoma cells and mouse B16F1 melanoma cells were supplied by the Yale University Skin Cancer SPORE. Normal human glia were derived from human temporal lobectomies, as previously described (Ozduman et al., 2008). Stably transfected cancer cells expressing red fluorescent protein (RFP) (rU87 and rYUMAC) were generated as described previously (Wollmann et al., 2013). rU373 and rU118 cells were generated using a lentiviral vector expressing RFP, then selected using G418. Vero cells were obtained from Dr. C. Cepko (Harvard University) and BHK-21 cells from Dr. J.K. Rose (Yale University). Mouse glia were isolated and cultured as previously described (van den Pol et al., 1992; van den Pol and Spencer, 2000). U87, 501mel, YUMAC, Vero, and mouse glia were maintained in MEM. BHK-21, U373, U118, CT-2A and human glia were maintained in DMEM. MDAMB-436, MDA-MB-231and BT-549 human breast cancer cells (from Dr.L.Pusztai, Yale University) were maintained in RPMI 1640. All culture media (MEM, DMEM, RPMI 1640; Gibco, Life Technologies, Grand Island, NY) was supplemented with 10% fetal bovine serum (Gibco) and 1% pen-strep solution (Gibco). All cells were maintained at 37 °C in an atmosphere supplemented with 5% CO_2.

Author Manuscript Author Manuscript Author Manuscript Author Manuscript

4.2. Viral plaque-size assay

We used a number of different cells including human glioblastoma U373, U118, U87 and mouse glioblastoma CT-2A, human normal glia, mouse glia, human melanoma YUMAC and 501mel, breast cancer MDAMB-436, MDA-MB-231 (Drs.L.Pusztai, V.Wali), BT-549 cells (ATCC, Manassas,VA) to study virus infection and replication.

To compare plaque sizes of VSVΔG-CHIKV on normal and multiple cancer cell types, cell monolayers were infected at an MOI of 0.02. Two hours later, inoculum was removed and cultures were washed 3 times with PBS before the addition of CMC in MEM, which was used as overlay. Three days later, plaques were determined by immunostaining. Plaque size was measured (n = 20 plaques/cell type/virus) and means and standard errors of the means (SEMs) were determined as an approach to compare infection and replication of VSVΔG-CHIKV.

To assess the capability of VSVΔG-CHIKV to propagate in glioblastoma cells, monolayer cultures of the cells were infected with CHIKV at an MOI of 0.02 (primary inoculation). Two hours later, virus inoculum was removed and cells were washed 3 times. After 24 h infection, all tumor lines showed infection as indicated by immunostaining with antisera against VSV. To test for viral propagation in these cells, supernatant was filtered (0.22 μm) and transferred to un-infected tumor dishes (secondary inoculation). Twenty-four hours later, positive immunofluorescence indicates transfer of viral progeny produced by tumors infected during primary inoculation. A recombinant hybrid type-I interferon IFN-α A/D (Sigma-Aldrich; catalog no. I4401) was used in some experiments.

4.3. Mouse procedures

Six- to seven-week-old immunodeficient adult CB17 SCID mice (Taconic Farms; Germantown, NY) were used for xenograft brain tumor models and postoperative care was performed in accordance with the institutional guidelines of the Yale University Animal Care and Use Committee. Tumors were established by unilateral striatal injection of 2 μl of cell suspension containing 2.5×10^4 cells/μl while mice were deeply anesthetized using a combination of ketamine and xylazine (100 and 10 mg/kg of body weight, respectively). Stereotactic intracerebral injections of tumor cells were made into the right striatum (2 mm lateral and 0.5 mm rostral to the bregma at 3 mm depth) using a micro-syringe (Hamilton Co., Reno, NV) controlled by a stereotactic injector (Stoelting Co., Wood Dale, IL). Eight days after tumor placement, mice received virus via intratumoral injection (3.0×10^8 PFU in 2 μl). For bilateral tumor implants, tumor cells were injected into the striatum or cortex (cortical coordinates: 2 mm lateral and 0.5 mm rostral to the bregma at 0.5 mm depth). For some histologic analyses of early states of viral infection, mice were sacrificed after viral inoculation by an anesthetic overdose followed by intracardiac perfusion with 4% paraformaldehyde. In some experiments, mice bearing tumors infected by VSVΔG-CHIKV were euthanized and tissue samples of tumor and control cerebellum were harvested. Tissue samples were dissociated into small pieces and the preparation was used to inoculate cultures of Vero cells to determine the presence or absence of viable virus.

Author Manuscript Author Manuscript Author Manuscript Author Manuscript

Mice were monitored daily and euthanized if any of the following conditions were observed: (i) weight loss of 25% or more, (ii) im-mobility, (iii) occurrence of adverse neurological symptoms, or (iv) reaching the end of the observation period of the survival study. Animal experiments were approved by and performed in accordance with the institutional guidelines of the Yale University Animal Care and Use Committee.

4.4. Immunocytochemistry

At the indicated time points, cells and brains were harvested and incubated in 4% (wt/vol) paraformaldehyde at 4 °C for 24 h. Brains were subsequently transferred into 30% (vol/vol) sucrose. In preparation for immunofluorescent labeling, brain sections were fixed in 4% paraformaldehyde, rinsed with phosphate-buffered saline (PBS), and permeabilized by washing 3 times for 10 min in PBS with 1% bovine serum albumin (BSA) and 0.4% Triton-X, blocked in washing buffer containing 2% normal horse serum (NHS), then exposed to primary antibody in blocking solution. A primary rabbit anti-wild type VSV antibody (Johnson et al., 1997) or rat anti-VSV antibody was used (overnight incubation; dilution 1:3000) to immunostain the sections. The VSV antibody binds to multiple VSV proteins, allowing detection of chimeric VSV viruses expressing non-VSV glycoproteins. After multiple washes to eliminate free primary antibody, a secondary goat anti-rabbit antibody conjugated to a green fluorescent molecule (Alexa Fluor 488; A11008; Invitrogen) or anti-rat secondary (2 h; dilution 1:1000) was used to localize the virus in infected cells. Finally, cells were incubated in nuclear stain Hoechst33342 (5 mg/ml in PBS) or, for cell death experiments, ethidium homodimer 1 (EthD-1; cat no. 40010; Biotium Inc, Fremont, CA) 2 μM in PBS for 20 min in the dark. Images were captured using a fluorescent microscope (Olympus IX71, Tokyo, Japan) fitted with a SPOT-RT camera (Diagnostic Instruments, Sterling Heights, MI). Contrast and brightness were corrected with universal application to the entire photograph using Adobe Photoshop.

4.5. Statistics

Statistical significance was analyzed by ANOVA; a p-value < 0.05 was considered significant. Kaplan-Meier survival curves and log-rank test were used to compare survival rates. Analysis was facilitated with the use of SPSS 19.0. The data are expressed as the mean ± SEM for each group.

Acknowledgements

We are indebted to John N. Davis and Yang Yang for excellent technical facilitation and suggestions on the manuscript, and Dr. R. Halaban and A. Bacchiocchi/Yale Skin Cancer SPORE for melanoma cells. Research support provided by NIH RO1- CA188359, CA161048, and CA175577.

References

Allen C, Paraskevakou G, Liu C, Iankov ID, Msaouel P, Zollman P, Myers R, Peng KW, Russell SJ, Galanis E, 2008 Oncolytic measles virus strains in the treatment of gliomas. Expert Opin. Biol. Ther 8, 213–220. [PubMed: 18194077]

Allen C, Opyrchal M, Aderca I, Schroeder MA, Sarkaria JN, Domingo E, Federspiel MJ, Galanis E, 2013 Oncolytic measles virus strains have significant antitumor activity against glioma stem cells. Gene Ther. 20, 444–449. [PubMed: 22914495]

Author Manuscript Author Manuscript Author Manuscript Author Manuscript

Amdekar S, Parashar D, Alagarasu K, 2017 Chikungunya virus-induced arthritis: role of host and viral factors in the pathogenesis. Viral Immunol. 30, 691–702. [PubMed: 28910194]

Banadyga L, Marzi A, 2017 Closer than ever to an Ebola virus vaccine. Expert Rev. Vaccin 16, 401–402.

Beier KT, Saunders A, Oldenburg IA, Miyamichi K, Akhtar N, Luo L, Whelan SP, Sabatini B, Cepko CL, 2011 Anterograde or retrograde transsynaptic labeling of CNS neurons with vesicular stomatitis virus vectors. Proc. Natl. Acad. Sci. USA 108, 15414–15419. [PubMed: 21825165]

Beier KT, Saunders AB, Oldenburg IA, Sabatini BL, Cepko CL, 2013 Vesicular stomatitis virus with the rabies virus glycoprotein directs retrograde transsynaptic transport among neurons in vivo. Front. Neural Circuits 7, 11. [PubMed: 23403489]

Bernard E, Solignat M, Gay B, Chazal N, Higgs S, Devaux C, Briant L, 2010 Endocytosis of chikungunya virus into mammalian cells: role of clathrin and early endosomal compartments. PLoS One 5, e11479. [PubMed: 20628602]

Cary ZD, Willingham MC, Lyles DS, 2011 Oncolytic vesicular stomatitis virus induces apoptosis in u87 glioblastoma cells by a type ii death receptor mechanism and induces cell death and tumor clearance in vivo. J. Virol 85 (5708–5717). [PubMed: 21450822]

Chandak NH, Kashyap RS, Kabra D, Karandikar P, Saha SS, Morey SH, Purohit HJ, Taori GM, Daginawala HF, 2009 Neurological complications of Chikungunya virus infection. Neurol. India 57, 177180.

Chattopadhyay A, Wang E, Seymour R, Weaver SC, Rose JK, 2013 A chimeric vesiculo/alphavirus is an effective alphavirus vaccine. J. Virol 87, 395–402. [PubMed: 23077320]

Clarke DK, Cooper D, Egan MA, Hendry RM, Parks CL, Udem SA, 2006 Recombinant vesicular stomatitis virus as an HIV-1 vaccine vector. Spring. Semin Immunopathol. 28, 239–253.

Das T, Jaffar-Bandjee MC, Hoarau JJ, Trotot PK, Denizot M, Lee-Pat-Yuen G, Sahoo R, Guiraud P, Ramful D, Robin S, Alessandri JL, Gauzere BA, Gasque P, 2010 Chikungunya fever: cns infection and pathologies of a re-emerging arbo-virus. Prog. Neurobiol 91, 121–129. [PubMed: 20026374]

Finkelshtein D, Werman A, Novick D, Barak S, Rubinstein M, 2013 LDL receptor and its family members serve as the cellular receptors for vesicular stomatitis virus. Proc. Natl. Acad. Sci. USA 110, 7306–7311. [PubMed: 23589850]

Galivo F, Diaz RM, Wongthida P, Thompson J, Kottke T, Barber G, Melcher A, Vile R, 2010 Single-cycle viral gene expression, rather than progressive replication and oncolysis, is required for VSV therapy of B16 melanoma. Gene Ther. 17, 158–170. [PubMed: 20016540]

Garbutt M, Liebscher R, Wahl-Jensen V, Jones S, Moller P, Wagner R, Volchkov V, Klenk H-D, Feldmann H, Stroher U, 2004 Properties of replication-competent vesicular stomatitis virus vectors expressing glycoproteins of filoviruses and arena-viruses. J. Virol 78, 5458–5465. [PubMed: 15113924]

Gasque P, 2013 Chikungunya virus infection In: Jackson AC (Ed.), Viral Infections of the Human Nervous System. Basel, Springer, pp. 295–315.

Geisbert TW, Daddario-DiCaprio KM, Lewis MG, Geisbert JB, Grolla A, Leung A, Paragas J, Matthias L, Smith MA, Jones SM, Hensley LE, Feldmann H, Jahrling PB, 2008 Vesicular stomatitis virus-based Ebola vaccine is well-tolerated and protects immunocompromised nonhuman primates. PLoS Pathog. 4, e1000225. [PubMed: 19043556]

Geisbert TW, Geisbert JB, Leung A, Daddario-DiCaprio KM, Hensley LE, Grolla A, Feldmann H, 2009 Single-injection vaccine protects nonhuman primates against infection with Marburg virus and three species of Ebola virus. J. Virol 83, 7296–7304. [PubMed: 19386702]

Hardcastle J, Mills L, Malo CS, Jin F, Kurokawa C, Geekiyanage H, Schroeder M, Sarkaria J, Johnson AJ, Galanis E, 2017 Immunovirotherapy with measles virus strains in combination with anti-PD-1 antibody blockade enhances antitumor activity in glioblastoma treatment. Neuro Oncol. 19, 493–502. [PubMed: 27663389]

Hoornweg TE, van Duijl-Richter MK, Ayala Nuñez NV, Albulescu IC, van Hemert MJ, Smit JM, 2016 Dynamics of chikungunya virus cell entry unraveled by single-virus tracking in living cells. J. Virol 90, 4745–4756. [PubMed: 26912616]

Hua C, Combe B, 2017 Chikungunya virus-associated disease. Curr. Rheumatol. Rep 19, 69. [PubMed: 28983760]

Author Manuscript Author Manuscript Author Manuscript Author Manuscript

Huneycutt BS, Bi Z, Aoki CJ, Reiss CS, 1993 Central neuropathogenesis of vesicular stomatitis virus infection of immunodeficient mice. J. Virol 67, 6698–6706. [PubMed: 8105106]

Jae LT, Raaben M, Riemersma M, van Beusekom E, Blomen VA, Velds A, Kerkhoven RM, Careyye JE, Topaloglu H, Meinecke P, Wessels MW, Lefeber DJ, Whelan SP, van Bokhoven H, Brummelkamp TR, 2013 Deciphering the glycosome of dystroglycanopathies using haploid screens for lassa virus entry. Science 340, 479–483. [PubMed: 23519211]

Johnson JE, Schnell MJ, Buonocore L, Rose JK, 1997 Specific targeting to $CD4^+$ cells of recombinant vesicular stomatitis viruses encoding human immunodeficiency virus envelope proteins. J. Virol 71, 5060–5068. [PubMed: 9188571]

Kurup D, Wirblich C, Feldmann H, Marzi A, Schnell MJ, 2015 Rhabdovirus-based vaccine platforms against henipaviruses. J. Virol 89, 144–154. [PubMed: 25320306]

Lawson ND, Stillman EA, Whitt MA, Rose JK, 1995 Recombinant vesicular stomatitis viruses from DNA. Proc. Natl. Acad. Sci. USA 92, 4477–4481. [PubMed: 7753828]

Lun X, Senger DL, Alain T, Oprea A, Parato K, Stojdl D, Lichty B, Power A, Johnston RN, Hamilton M, Parney I, Bell JC, Forsyth PA, 2006 Effects of intravenously administered recombinant vesicular stomatitis virus (VSV(deltaM51)) on multifocal and invasive gliomas. J. Natl. Cancer Inst. 98, 1546–1557. [PubMed: 17077357]

Lundh B, Kristensson K, Norrby E, 1987 Selective infections of olfactory and respiratory epithelium by vesicular stomatitis and Sendai viruses. Neuropathol. Appl. Neurobiol 13, 111–122. [PubMed: 3039392]

Lundh B, Löve A, Kristensson K, Norrby E, 1988 Non-lethal infection of aminergic reticular core neurons: age-dependent spread of ts mutant vesicular stomatitis virus from the nose. J. Neuropathol. Exp. Neurol 47, 497–506. [PubMed: 2845000]

Lyles DS, Rupprecht CE, 2007 Rhabdoviridae In: Knipe DM, Howley PM (Eds.), Fields Virology, 5th ed. Lippincott Williams and Wilkins, Philadelphia, PA, pp. 1363–1408.

Marzi A, Robertson SJ, Haddock E, Feldmann F, Hanley PW, Scott DP, Strong JE, Kobinger G, Best SM, Feldmann H, 2015 EBOLA VACCINE. VSV-EBOV rapidly protects macaques against infection with the 2014/15 Ebola virus outbreak strain. Science 349, 739–742. [PubMed: 26249231]

Marzi A, Hanley PW, Haddock E, Martellaro C, Kobinger G, Feldmann H, 2016 Efficacy of Vesicular Stomatitis Virus-Ebola Virus postexposure treatment in Rhesus Macaques Infected With Ebola Virus Makona. J. Infect. Dis 214, S360–S366. [PubMed: 27496978]

Mire CE, Miller AD, Carville A, Westmoreland SV, Geisbert JB, Mansfield KG, Feldmann H, Hensley LE, Geisbert TW, 2012 Recombinant vesicular stomatitis virus vaccine vectors expressing filovirus glycoproteins lack neurovirulence in non-human primates. PLoS Negl. Trop. Dis. 6, e1567. [PubMed: 22448291]

Muik A, Kneiske I, Werbizki M, Wilflingseder D, Giroglou T, Ebert O, Kraft A, Dietrich U, Zimmer G, Momma S, von Laer D, 2011 Pseudotyping vesicular stomatitis virus with lymphocytic choriomeningitis virus glycoproteins enhances infectivity for glioma cells and minimizes neurotropism. J. Virol 85, 5679–5684. [PubMed: 21450833]

Naik S, Leblanc AK, Galyon G, Frazier S, Jenks N, Steele M, Miller A, Peng KW, Federspiel M, Russell SJ, 2015 Safety, toxicity and efficacy of systemic recombinant VSV therapy in pet dogs with spontaneous cancer. Mol. Ther 23 (Suppl.1), S30–S31.

Obuchi M, Fernandez M, Barber GN, 2003 Development of recombinant vesicular stomatitis viruses that exploit defects in host defense to augment specific oncolytic activity. J. Virol 77, 8843–8856. [PubMed: 12885903]

Ozduman K, Wollmann G, Piepmeier JM, van den Pol AN, 2008 Systemic vesicular stomatitis virus selectively destroys multifocal glioma and metastatic carcinoma in brain. J. Neurosci 28, 1882–1893. [PubMed: 18287505]

Ozduman K, Wollmann G, Ahmadi SA, van den Pol AN, 2009 Peripheral immunization blocks lethal actions of vesicular stomatitis virus within the brain. J. Virol 83, 11540–11549. [PubMed: 19726512]

Pinheiro TJ, Guimaraes LF, Silva MT, Soares CN, 2016 Neurological manifestations of Chikungunya and Zika infections. Arq. Neuropsychol 74, 937–943.

Author Manuscript Author Manuscript Author Manuscript Author Manuscript

Powers AM, 2018 Vaccine and therapeutic options to control chikungunya virus. Clin. Microbiol. Rev 31, e00104–e00116. [PubMed: 29237708]

Powers AM, Logue CH, 2007 Changing patterns of Chikungunya virus: reemergence of a zoonotic arbovirus. J. Gen. Virol 88, 2363–2377. [PubMed: 17698645]

Rose NF, Marx PA, Luckay A, Nixon DF, Moretto WJ, Donahoe SM, Montefiori D, Roberts A, Buonocore L, Rose JK, 2001 An effective AIDS vaccine based on live attenuated vesicular stomatitis virus recombinants. Cell 106, 539–549. [PubMed: 11551502]

Schwartz O, Albert ML, 2010 Biology and pathogenesis of chikungunya virus. Nat. Rev. Microbiol. 8, 491–500. [PubMed: 20551973]

Solignat M, Gay B, Higgs S, Briant L, Devaux C, 2009 Replication cycle of chikungunya: a re-emerging arbovirus. Virology 393, 183–197. [PubMed: 19732931]

Stojdl DF, Lichty B, Knowles S, Marius R, Atkins H, Sonenberg N, Bell JC, 2000 Exploiting tumor-specific defects in the interferon pathway with a previously unknown oncolytic virus. Nat. Med 6, 821–825. [PubMed: 10888934]

Taylor A, Melton JV, Herrero LJ, Thaa B, Karo-Astover L, Gage PW, Nelson MA, Sheng KC, Lidbury BA, Ewart GD, McInerney GM, Merits A, Mahalingam S, 2016 Effects of an in-frame deletion of the 6k gene locus from the genome of Ross River virus. J. Virol 90, 4150–4159. [PubMed: 26865723]

Uchime O, Fields W, Kielian M, 2013 The role of E3 in pH protection during alphavirus assembly and exit. J. Virol 87, 10255–10262. [PubMed: 23864626]

van den Pol AN, Davis JN, 2013 Highly attenuated recombinant vesicular stomatitis virus VSV-12′GFP displays immunogenic and oncolytic activity. J. Virol 87, 1019–1034. [PubMed: 23135719]

van den Pol AN, Spencer DD, 2000 Differential neurite growth on astrocyte substrates: interspecies facilitation in green fluorescent protein-transfected rat and human neurons. Neuroscience 95, 603–616. [PubMed: 10658640]

van den Pol AN, Finkbeiner SM, Cornell-Bell AH, 1992 Calcium excitability and oscillations in suprachiasmatic nucleus neurons and glia in vitro. J. Neurosci 12, 2648–2664. [PubMed: 1351936]

van den Pol AN, Dalton KP, Rose JK, 2002 Relative neurotropism of a recombinant rhabdovirus expressing a green fluorescent envelope glycoprotein. J. Virol 76, 1309–1327. [PubMed: 11773406]

van den Pol AN, Ding S, Robek MD, 2014 Long distance interferon signaling within the brain blocks virus spread. J. Virol 88, 3695–3704. [PubMed: 24429359]

van den Pol AN, Mao G, Chattopadhyay A, Rose JK, Davis JN, 2017a Chikungunya, Influenza, Nipah, and Semliki Forest chimeric viruses with vesicular stomatitis virus: actions in the brain. J. Virol 91 (e02154–16). [PubMed: 28077641]

van den Pol AN, Mao G, Yang Y, Ornaghi S, Davis JN, 2017b Zika virus targeting in the developing brain. J. Neurosci 37, 2161–2175. [PubMed: 28123079]

Vignuzzi M, Higgs S, 2017 The bridges and blockades to evolutionary convergence on the road to predicting chikungunya virus evolution. Annu. Rev. Virol 4, 181–200. [PubMed: 28961411]

Voss JE, Vaney M-C, Duquerroy S, Vonrhein C, Girard-Blanc C, Crublet E, Thompson A, Bricogne G, Rey FA, 2010 Glycoprotein organization of Chikungunya virus particles revealed by X-ray crystallography. Nature 468, 709–712. [PubMed: 21124458]

Vu DM, Jungkind D, Angelle Desiree L, 2017 Chikungunya Virus. Clin. Lab Med 37, 371–382. [PubMed: 28457355]

Wei B, Wang L, Du C, Hu G, Wang L, Jin Y, Kong D, 2015 Identification of differentially expressed genes regulated by transcription factors in glioblastomas by bioinformatics analysis. Mol. Med. Rep 11, 2548–2554. [PubMed: 25514975]

Wichit S, Hamel R, Bernard E, Talignani L, Diop F, Ferraris P, Liegeois F, Ekchariyawat P, Luplertlop N, Surasombatpattana P, Thomas F, Merits A, Choumet V, Roques P, Yssel H, Briant L, Missé D, 2017 Imipramine inhibits chikungunya virus replication in human skin fibroblasts through interference with intracellular cholesterol trafficking. Sci. Rep 7, 3145. [PubMed: 28600536]

Wintachai P, Wikan N, Kuadkitkan A, Jaimipuk T, Ubol S, Pulmanausahakul R, Auewarakul P, Kasinrerk W, Weng W-Y, Panyasrivanit M, Paemanee A, Kittisenachai S, Roytrakul S, Smith DR,

Author Manuscript Author Manuscript Author Manuscript Author Manuscript

2012 Identification of prohibitin as a Chikungunya virus receptor protein. J. Med. Virol 84, 1757–1770. [PubMed: 22997079]

Wollmann G, Tattersall P, van den Pol AN, 2005 Targeting human glioblastoma cells: comparison of nine viruses with oncolytic potential. J. Virol 79, 6005–6022. [PubMed: 15857987]

Wollmann G, Ozduman K, van den Pol AN, 2012 Oncolytic virus therapy for glioblastoma multiforme: concepts and candidates. Cancer J. 18, 69–81. [PubMed: 22290260]

Wollmann G, Davis JN, Bosenberg MW, van den Pol AN, 2013 Vesicular stomatitis virus variants selectively infect and kill human melanomas but not normal melanocytes. J. Virol 87, 6644–6659. [PubMed: 23552414]

Wollmann G, Drokhlyansky E, Davis JN, Cepko C, van den Pol AN, 2015 Lassavesicular stomatitis chimeric virus safely destroys brain tumors. J. Virol 89, 6711–6724. [PubMed: 25878115]

Wongthida P, Diaz RM, Pulido C, Rommelfanger D, Galivo F, Kaluza K, Kottke T, Thompson J, Melcher A, Vile R, 2011 Activating systemic T-cell immunity against self tumor antigens to support oncolytic virotherapy with vesicular stomatitis virus. Hum. Gene Ther. 22, 1343–1353. [PubMed: 21366404]

Yang S, Fink D, Hulse A, Pratt RD, 2017 Regulatory considerations in development of vaccines to prevent disease caused by Chikungunya virus. Vaccine 35, 4851–4858. [PubMed: 28760614]

Yarde DN, Naik S, Nace RA, Peng KW, Federspiel MJ, Russell SJ, 2013 Meningeal myeloma deposits adversely impact the therapeutic index of an oncolytic VSV. Cancer Gene Ther. 20, 616–621. [PubMed: 24176894]

Zhang L, Steele MB, Jenks N, Grell J, Suksanpaisan L, Naik S, Federspiel MJ, Lacy MQ, Russell SJ, Peng KW, 2016a Safety studies in tumor and non-tumor-bearing mice in support of clinical trials using oncolytic VSV-IFNβ-NIS. Hum. Gene Ther. Clin. Dev 27, 111–122. [PubMed: 27532609]

Zhang L, Steele MB, Jenks N, Grell J, Behrens M, Nace R, Naik S, Federspiel MJ, Russell SJ, Peng KW, 2016b Robust oncolytic virotherapy induces tumor lysis syndrome and associated toxicities in the mpc-11 plasmacytoma model. Mol. Ther 24, 2109–2117. [PubMed: 27669655]

Ziegler SA, Lu L, da Rosa AP, Xiao SY, Tesh RB, 2008 An animal model for studying the pathogenesis of Chikungunya virus infection. Am. J. Trop. Med. Hyg 79, 133–139. [PubMed: 18606777]

Author Manuscript Author Manuscript Author Manuscript Author Manuscript

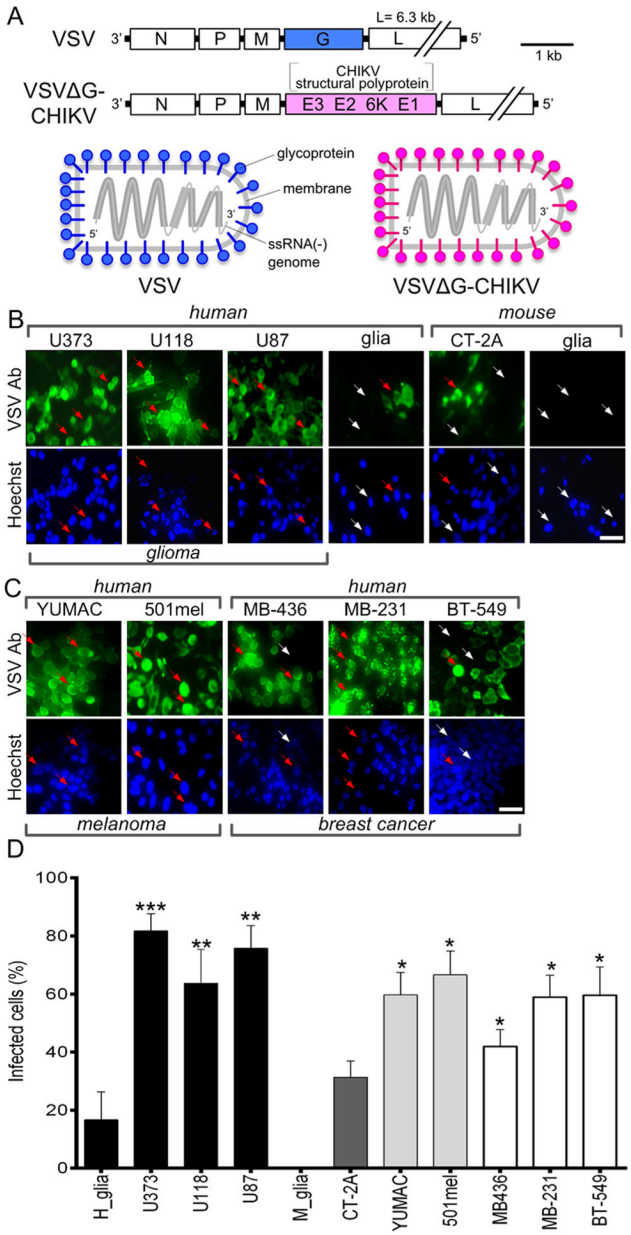

Fig. 1. Chimeric VSVΔG-CHIKV infects glioblastoma, melanoma, and breast cancer cells.

A. Schematic illustration (top) showing genomes of wild-type VSV and chimeric VSVΔG-CHIKV in which the VSV glycoprotein G gene (blue) has been replaced with the chikungunya glycoprotein sequence from the CHIKV structural polyprotein (pink). The diagram below illustrates this replacement in assembled viral particles. **B.** VSVΔG-CHIKV (MOI 0.02) was used to infect a collection of glioma cell lines from human (U373, U118, U87) and mouse (CT-2A) along with primary cultures of human glia and mouse glia. 3 days post infection (3 dpi), cells were visualized by immunolabeling with a primary antibody against VSV together with a secondary fluorescent antibody; cells were also stained with blue Hoechst33342 nuclear stain. Arrows indicate infected (red arrow) and uninfected (white arrow) cells. C. Infection of human melanoma (YUMAC, 501mel) and breast cancer (MDA-

Author Manuscript Author Manuscript Author Manuscript Author Manuscript

MB-436, MDA-MB-231, BT-549) cells 3 dpi. Scale bars 50 μm. **D.** VSVΔG-CHIKV (MOI 0.02) was used to test infection of human glioma cells (U373, U118, U87), mouse glioma (CT-2A), primary cultures of normal human glia and mouse glia, human melanoma (YUMAC, 501mel) and human breast cancer (MDA-MB-436, MDA-MB-231, BT-549) cells, 3 days post infection (3 dpi). Uninfected cells are identified with phase contrast microscopy. Statistical comparisons are between tumor cells and the normal human cells (glia). Values are reported as the mean ± SEM; n = 6. *$p < 0.05$, * *$p < 0.01$, * **$p < 0.001$ one-way ANOVA with repeated measures.

Author Manuscript Author Manuscript Author Manuscript Author Manuscript

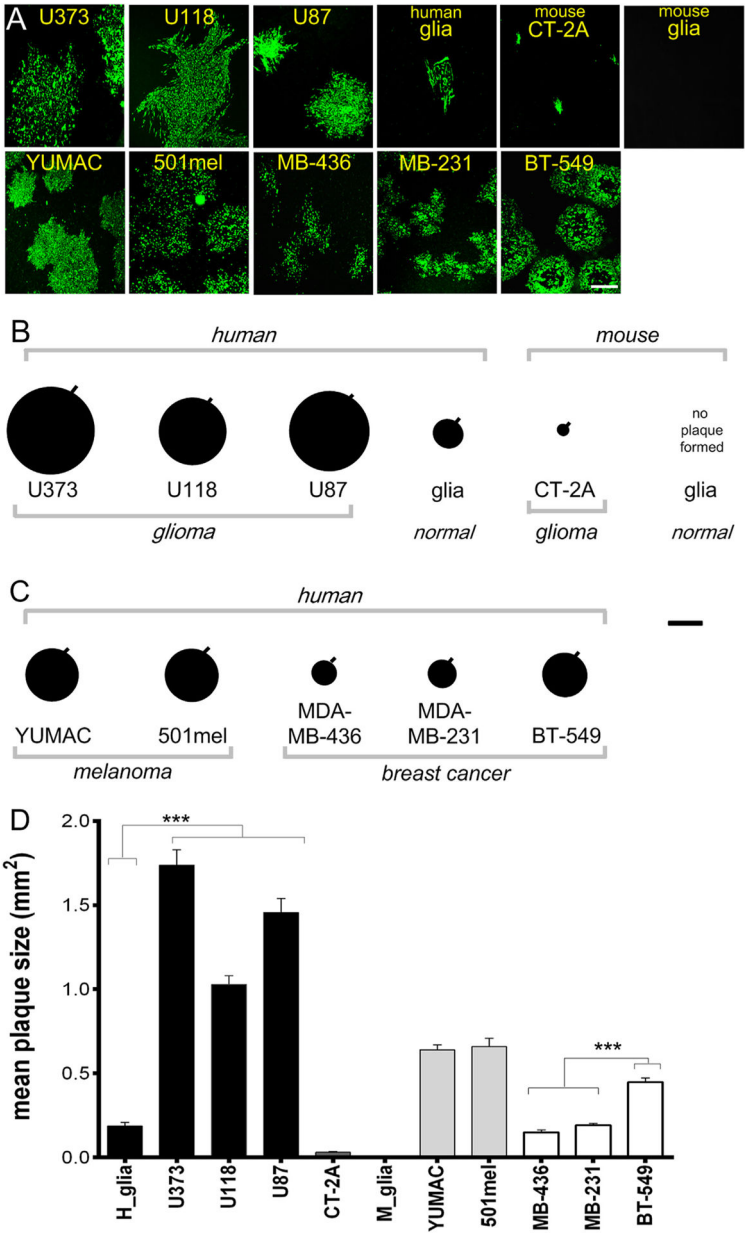

Fig. 2. Glioblastoma cells generate larger VSVΔG-CHIKV plaques than cultures of normal human glia.

A. Representative immunofluorescent images of viral plaques that developed 3 days post infection of monolayer cultures of human glioma (U373, U118, U87), mouse glioma (CT-2A), human melanoma (YUMAC, 501mel), human breast cancer cells (MDA-MB-436, MDA-MB-231, BT-549), and normal human glia (H glia) and mouse glia (M glia). Scale bar 0.5 mm. **B.** Plaque size was measured as an indicator of viral propagation in human and mouse glioma. Each black circle shows the mean size of 20 randomly selected plaques with the SEM indicated by the black line on the upper right of each circle. **C.** Plaque sizes measured in human melanoma and breast cancer cells. Scale bar 0.6 mm. **D.** The bar graph shows the mean plaque size. Values are reported as the mean +/− SEM; n = 20. ***p < 0.001, one-way ANOVA with repeated measures.

Author Manuscript Author Manuscript Author Manuscript Author Manuscript

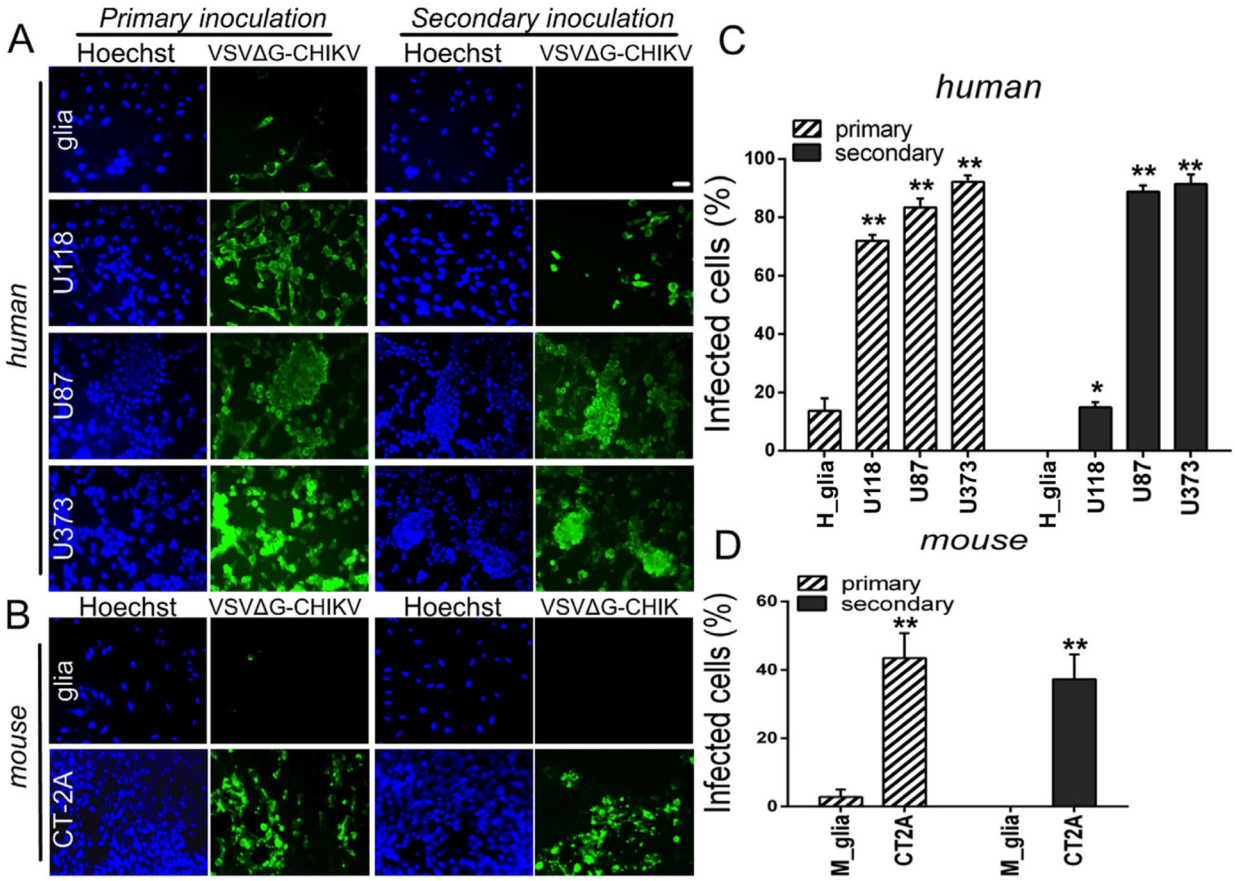

Fig. 3. VSVΔG-CHIKV replicates in mouse and human glioblastoma cells.

A. Monolayer cultures of human glioblastoma cells were infected with VSVΔG-CHIKV at an MOI of 0.02 (*primary inoculation*). Two hours later, virus inoculum was removed and cells were washed 3 times with PBS. 24 hrs later, all glioblastoma cell types were robustly infected, as indicated by immunofluorescent labeling with the VSV antibody. Cell nuclei are labeled blue with Hoechst33342 dye. To test for viral propagation, media was collected from these cultures and filtered (0.22 μm filter) before transferring to fresh cultures of uninfected cells (*secondary inoculation*). 24 hrs later, immunofluorescent labeling indicates infectious transmission of viral progeny generated by cultures during the primary inoculation. B. The same experiment performed using mouse CT-2A cells and primary mouse glia. Scale bar 100 μm. C. and D. The bar graph shows the percentage of infected cells. Values are reported as the mean ± SEM; n = 6. *$p < 0.05$, * *$p < 0.01$ vs. normal cells; one-way ANOVA with repeated measures.

Author Manuscript Author Manuscript Author Manuscript Author Manuscript

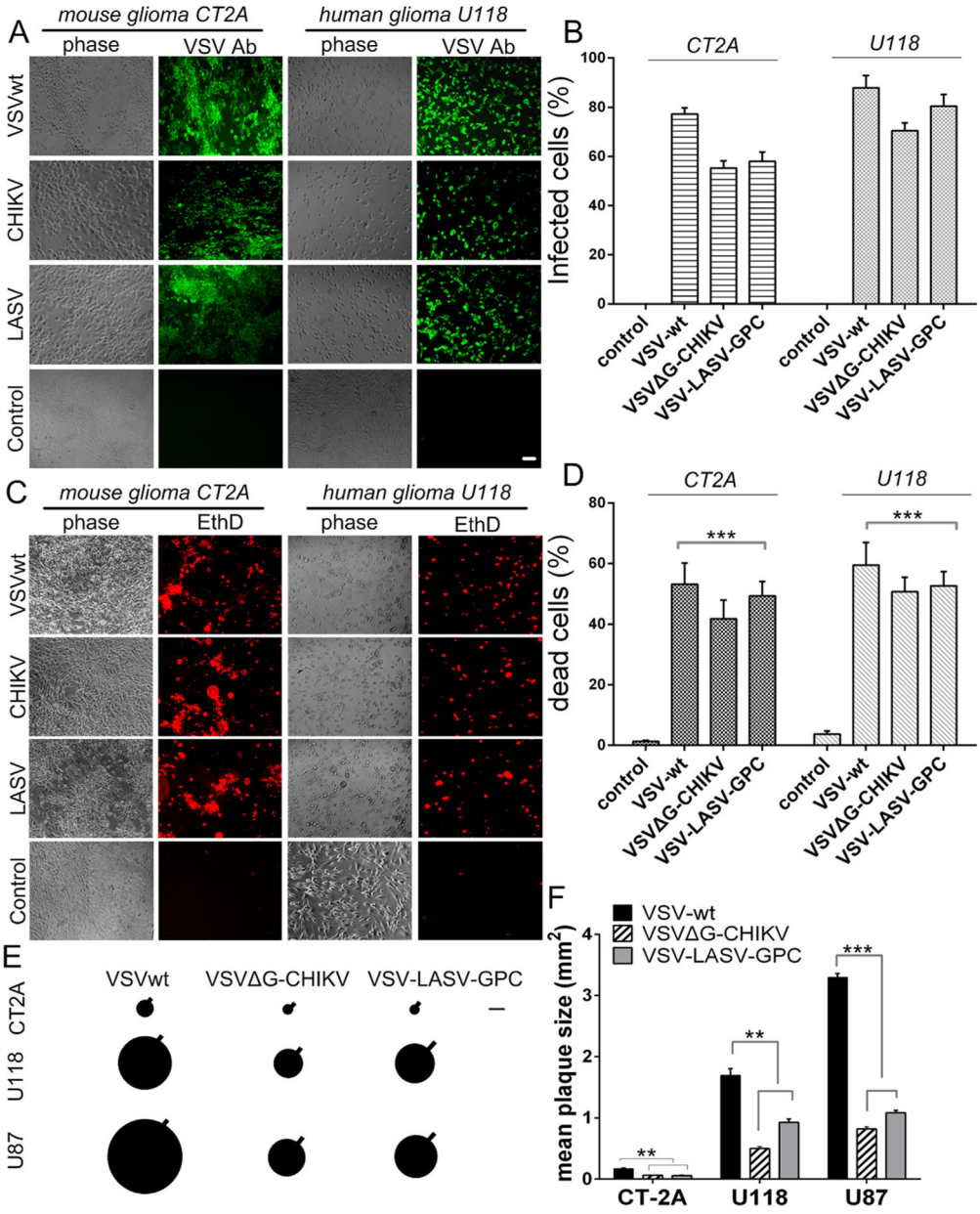

Fig. 4. Comparison of VSVΔG-CHIKV with two additional recombinant VSVs. A–D.
VSVΔG-CHIKV, VSVwt and VSV-LASV-GPC (MOI 1) were used to infect glioma cells derived from human (U118) and mouse (CT-2A). A,B. One day post-infection, cells were visualized by immunolabeling (green) with a primary antibody against VSV together with a secondary fluorescent antibody. C,D. Prior to immunolabeling, dead cells were labeled (red) using ethidium homodimer 1 (EthD). Bar graphs display mean percentage ± SEM of indicated cell counts; n = 6 and * **p < 0.001 one-way ANOVA with repeated measures. **E.** Diagram showing the relative size of viral plaques that developed 48 h post-infection on monolayer cultures of human (U118, U87) and mouse (CT-2A) glioma cells using VSVΔG-CHIKV, VSVwt and VSV-LASV-GPC. Each circle depicts the mean plaque size of 20 randomly selected plaques; the SEM is indicated by the black line projecting from each.

Author Manuscript Author Manuscript Author Manuscript Author Manuscript

Scale bar 0.55 mm. **F.** Bar graph shows mean plaque sizes in mm^2 ± SEM; n = 20. **p < 0.01, ***p < 0.001, one way ANOVA with repeated measures.

Author Manuscript Author Manuscript Author Manuscript Author Manuscript

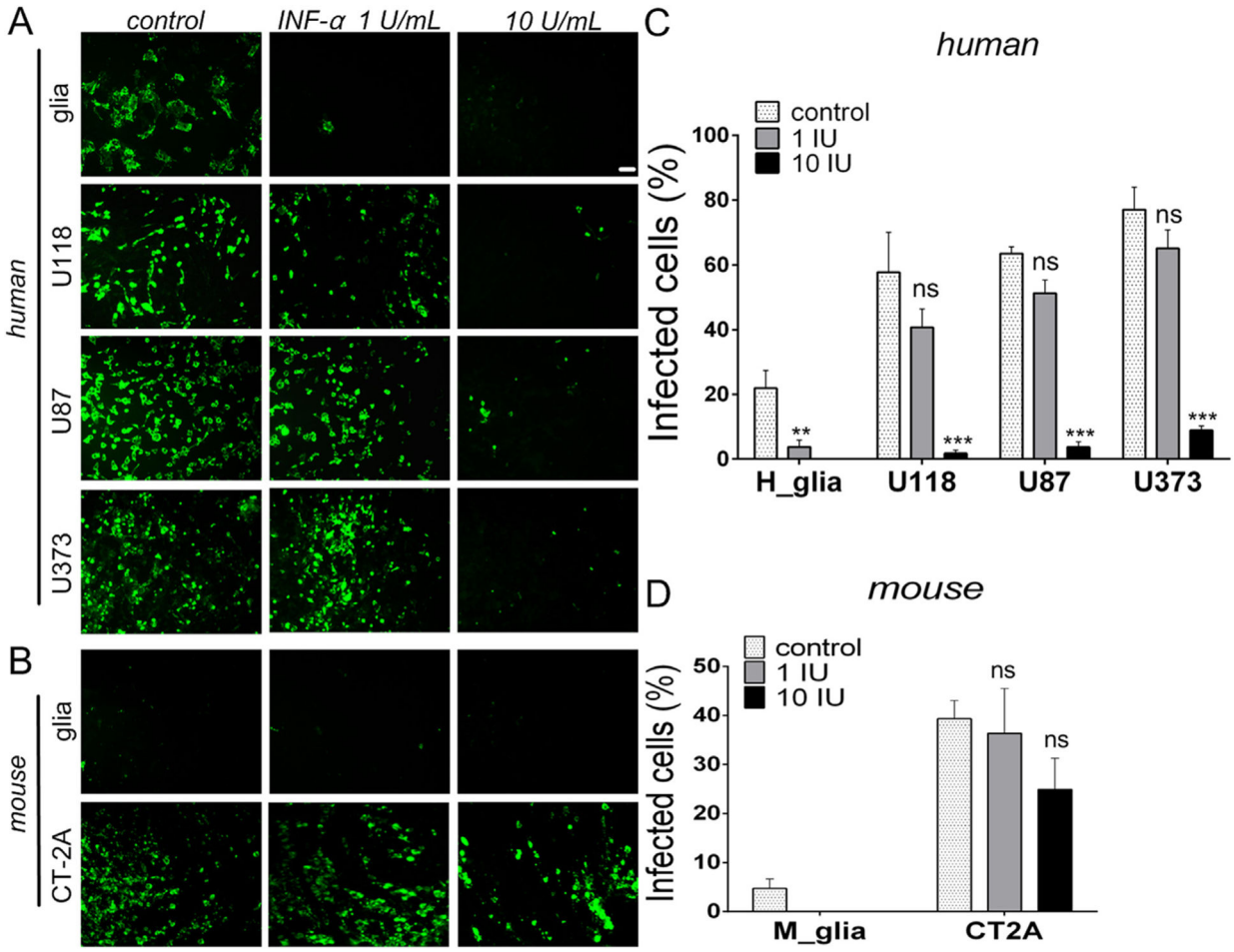

Fig. 5. Type I IFN-α inhibits VSVΔG-CHIKV.

A. Human cells were pretreated with a recombinant hybrid type-I interferon, IFN-α A/D (Sigma-Aldrich I4401), at different concentrations (0, 1 and 10 IU/ml) for 12 h prior to infection with VSVΔG-CHIKV at an MOI of 0.02. Despite IFN-α treatment, strong viral infection was seen in glioma cells at 24 hpi. Infected cells were visualized by immunofluorescent labeling with VSV immunostaining. Scale bar 0.1 mm. **B.** The same experiment was also performed with mouse CT-2A cells compared with primary mouse glia. **C. and D.** The bar graph shows the percentage of infected cells. Values are reported as the mean ± SEM; n = 6. ns, not significant, * *p < 0.01, * **p < 0.001 vs. control; ANOVA with repeated measures.

Author Manuscript Author Manuscript Author Manuscript Author Manuscript

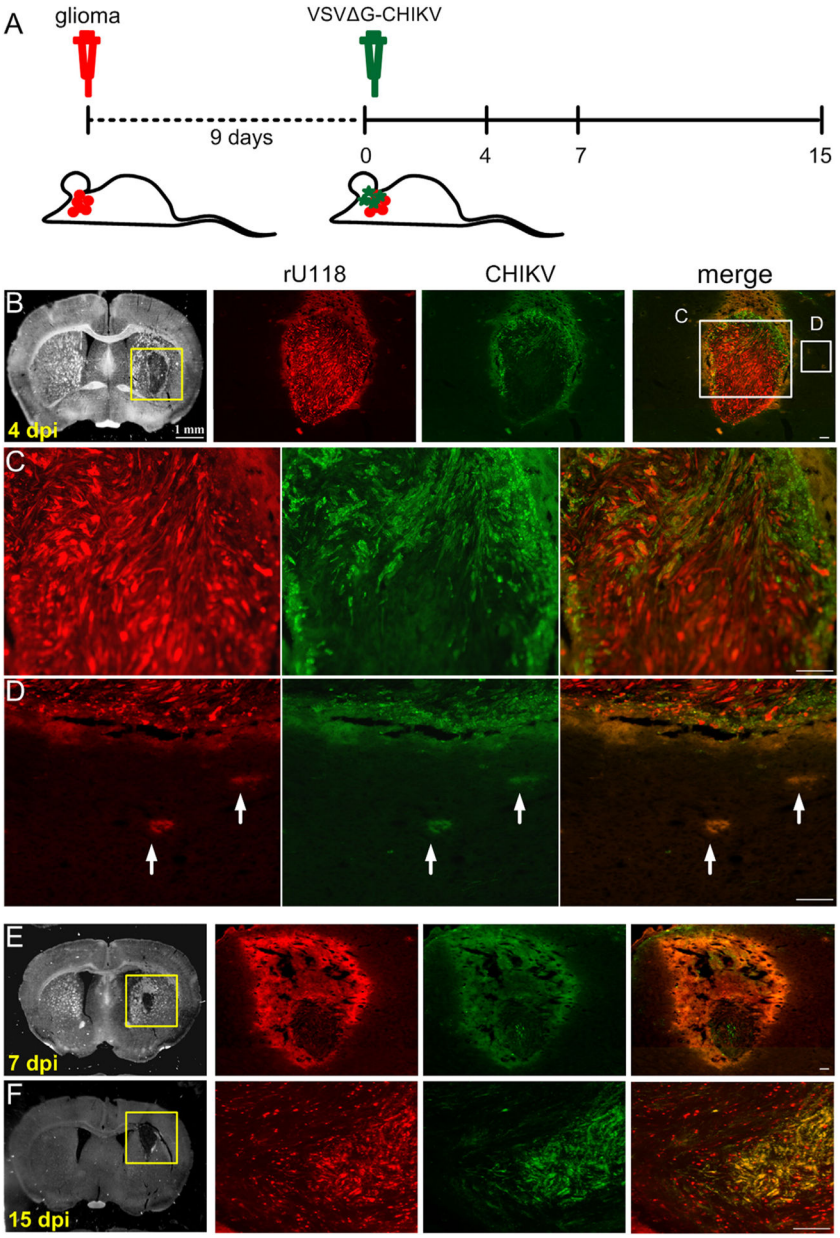

Fig. 6. VSVΔG-CHIKV targets additional U118 glioma in brain.

CB17 SCID mice with unilateral striatal xenografts of human RFP-expressing rU118 glioma (n = 3) were treated with a single intracranial injection of VSVΔG-CHIKV 9 days after tumor placement. Mice were euthanized 4, 7 and 15 days later. **A.** Schematic illustration outlining the in vivo experimental procedure. The glioma rU118 expresses red fluorescent protein reporter. VSVΔG-CHIKV was detected by green immunofluorescent labeling. **B.-F.** Infection. Arrows (white) indicate infected cells. The virus selectively infected the red glioma cells at all stages from 4 to 15 dpi. Scale bar, (B) 1 mm, and (B merge,C,D,E,F) 0.1 mm.

Author Manuscript Author Manuscript Author Manuscript Author Manuscript

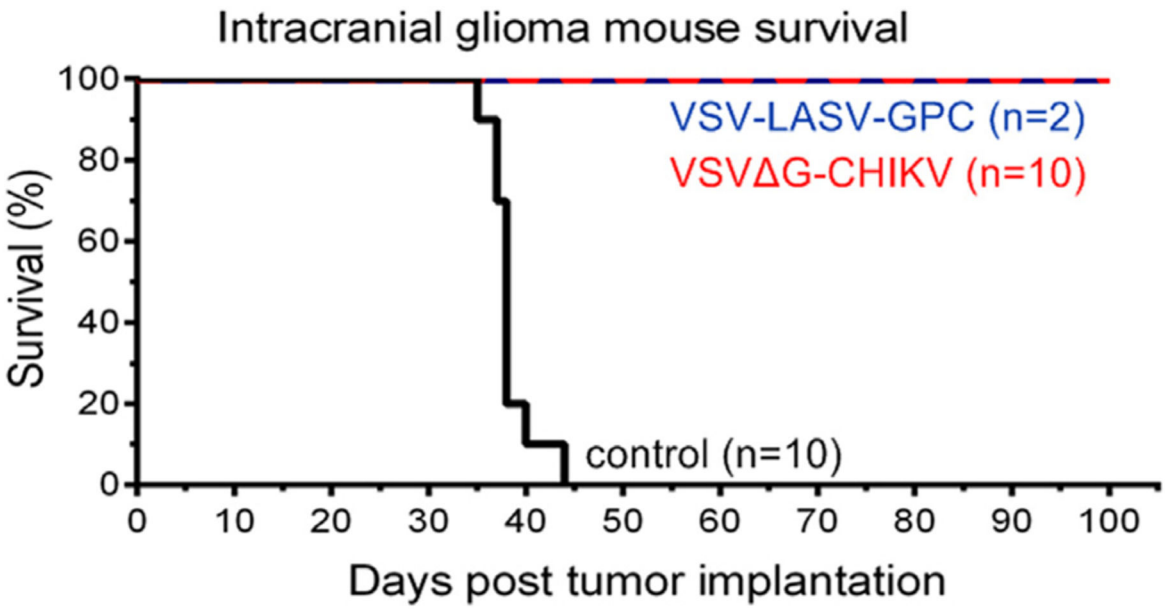

Fig. 7. Intracranial VSVΔG-CHIKV destroys brain glioma and enhances survival.

CB17 SCID mice with unilateral striatal xenografts of human rU87 glioma expressing RFP were treated with a single intracranial injection of either VSVΔG-CHIKV, VSV-LASV-GPC (2 μl of 3.0 $\times 10^8$ PFU for each) or saline (control) 8 days after tumor implantation. VSVΔG-CHIKV-treated mice (n = 10) showed complete survival throughout the observation period (100 days) compared to untreated control (n = 10 each), and there was no obvious difference between VSVΔG-CHIKV-treated mice and VSV-LASV-GPC-treated mice.

Author Manuscript Author Manuscript Author Manuscript Author Manuscript

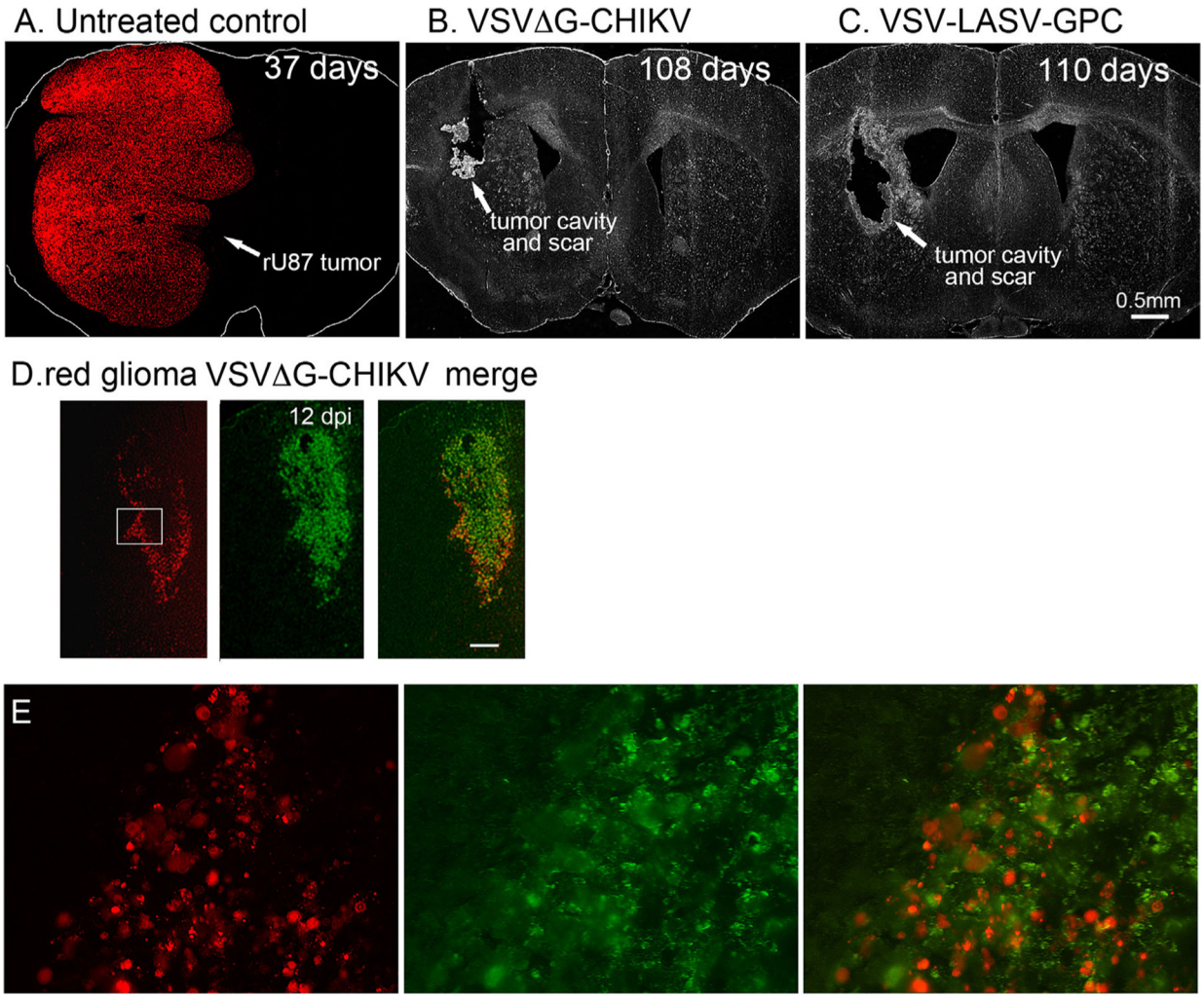

Fig. 8. VSVΔG-CHIKV selectively infects glioma within the brain.

The panel displays representative brain sections for U87 tumor-bearing controls (n = 10) and virus-treated tumor-bearing mice (n = 10) from brains in Fig. 7. **A.** Brains from untreated control mice showed massive expansion of the tumor mass (red), causing a significant midline shift of the longitudinal cerebral fissure. Number of days after tumor implantation is indicated. No green fluorescence was detected. B. VSVΔG-CHIKV eliminated tumors, as shown by the lack of red tumor cells. Histological analysis showed no residual viable tumor mass, only scar tissue and a tumor cavity, indicating successful oncolysis. **C.** Intracranial VSV-LASV-GPC eliminated tumors. No green fluorescence was detected in B or C indicating the absence of detectable virus immunofluorescence. **D.** Mouse treated with VSVΔG-CHIKV showed selective infection in tumor when euthanized at 12 dpi. Red tumor on left, green immunofluorescence showing VSVΔG-CHIKV in middle, merge of the two images on the right. Scale, 150 μm. **E.** Higher magnification of an area within the white rectangle in **D.** VSVΔG-CHIKV caused widespread oncolysis in the central portions of glioma tumors with dead or dying cells. Infection was restricted to the tumor.

Author Manuscript Author Manuscript Author Manuscript Author Manuscript

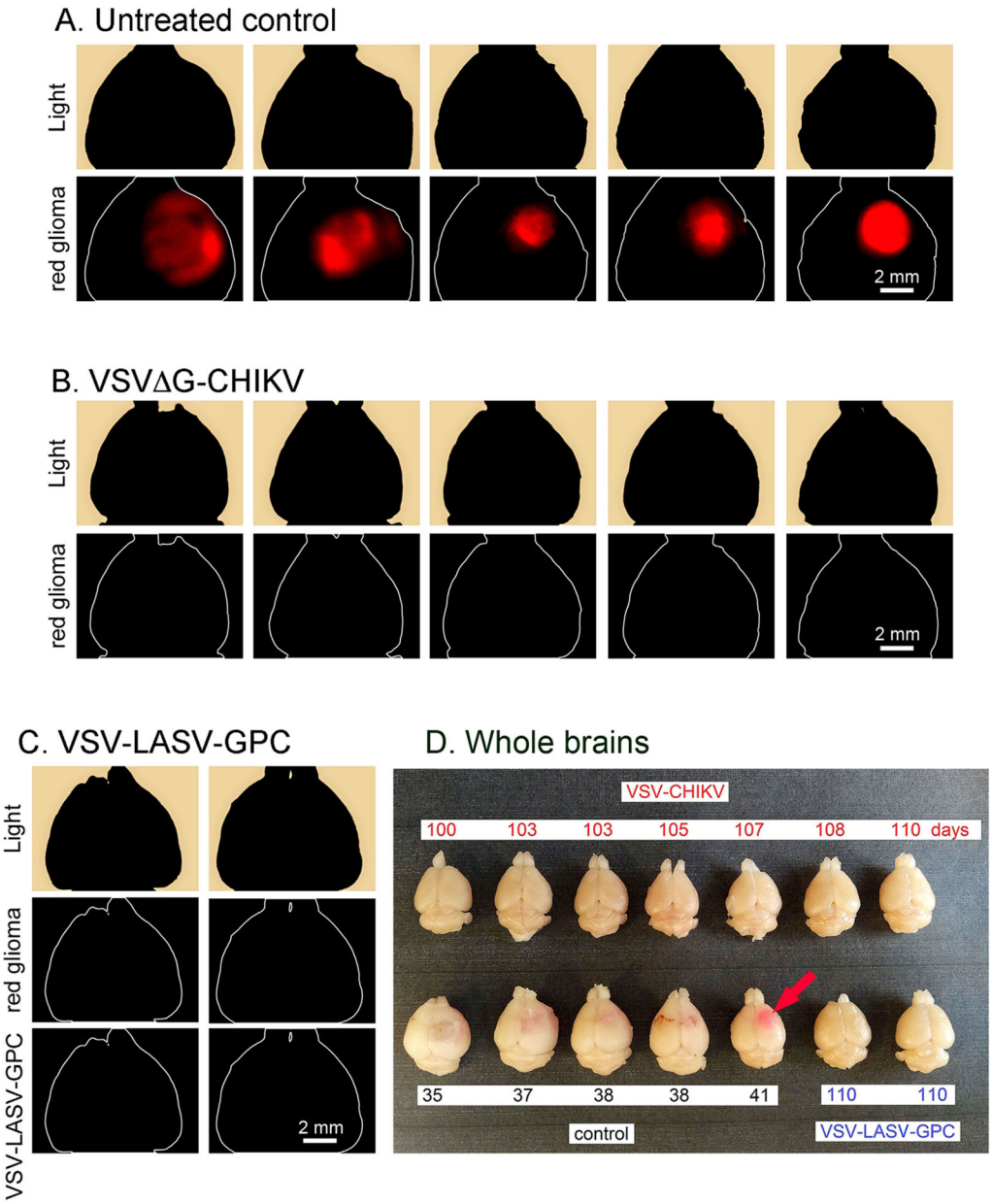

Fig. 9. VSVΔG-CHIKV destroys brain glioma.

(A, B, and C) Analysis for expression of red U87 glioma fluorescence revealed a consistently bright fluorescent signal on the injected side. Images show a dorsal view of uncut brains of mice taken with an Olympus fluorescence microscope from brains related to Fig. 7**A.** Untreated control mice (n = 5). **B.** Mouse brains after treatment with VSVΔG-CHIKV show no detectable red tumor from dorsal view. **B–C.** Two brains from tumor-bearing mice treated with VSV-LASV-GPC do not show detectable red tumor. **D.** The panel displays representative brains for each group. Brains from untreated control mice showed large expansion of the tumor mass (pink, pink arrow) causing a midline shift of the longitudinal cerebral fissure. In contrast, brains from VSVΔG-CHIKV or VSV-LASV-GPC-

Author Manuscript Author Manuscript Author Manuscript Author Manuscript

treated mice showed no visible expansion of the brain at the end of the observation period. These observations suggest successful tumor oncolysis compared to untreated control.

Author Manuscript Author Manuscript Author Manuscript Author Manuscript

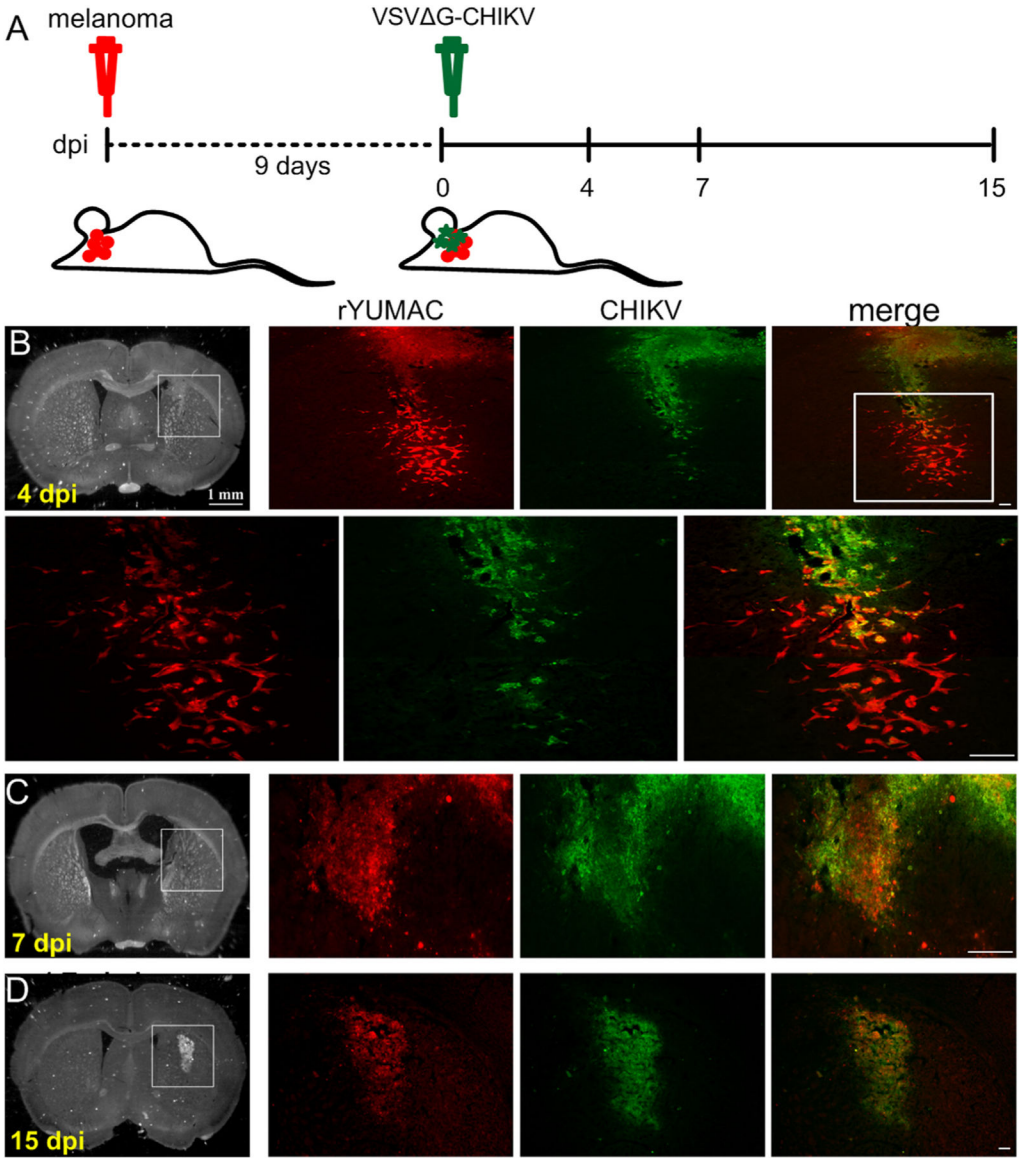

Fig. 10. VSVΔG-CHIKV targets melanoma in brain.

A. Schematic shows time course of in vivo experiments (n = 3). VSVΔG-CHIKV (green) was detected by immunostaining. **B–D.** Selective Infection of red human melanoma cells (YUMAC) within the brain at 4 dpi (B), 7 dpi (C), and 15 dpi (D). Scale bar, 1 mm, 0.5 mm and 0.1 mm.

Author Manuscript
Author Manuscript
Author Manuscript
Author Manuscript

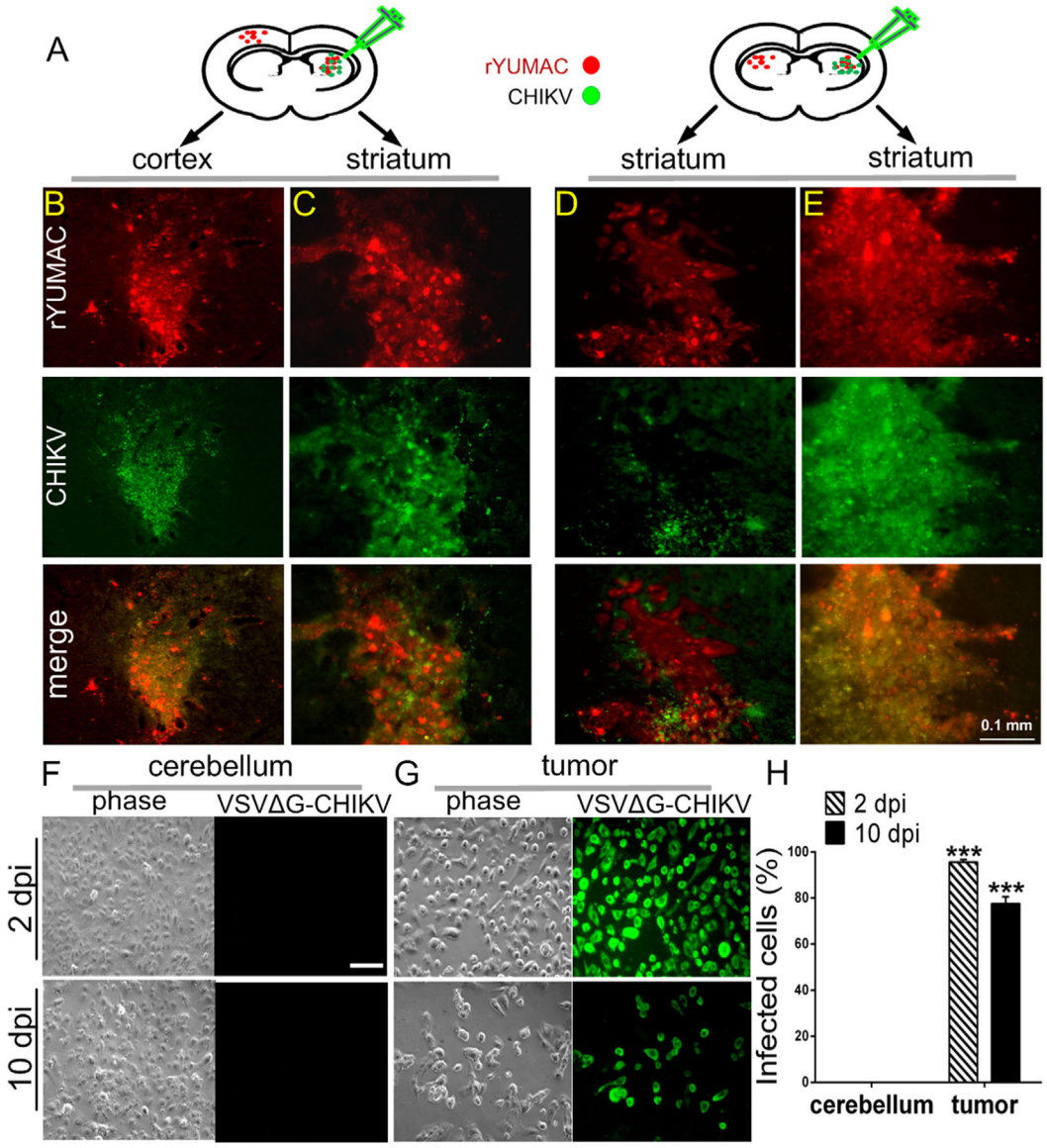

Fig. 11. VSVΔG-CHIKV infects distant brain tumors in metastasis model.

A. CB17 SCID mice (n = 5) received bilateral xenografts of rYUMAC melanoma cells expressing RFP. 8 days later, only the tumor on the right side was injected stereotactically with 1 μl (7×10^5 PFU) of VSVΔG-CHIKV. Brains were harvested 8 days later. **B, C.** Both red (tumor) and green (virus infection) fluorescence were detected in the injected right striatum (C) and in the non-injected left cortex (B). **D, E.** Analysis of expression of RFP (tumor) and virus immunofluorescence revealed strong viral fluorescence in the right injected striatal tumor (E) and also showed fluorescence associated with the left non-injected striatal tumor in the side of the brain contralateral to the virus injection (D). Scale bar, 0.1 mm. **F–H.** CB17 SCID mice (n = 3) received bilateral xenografts of rYUMAC melanoma cells expressing RFP. 10 days later, 0.5 μl VSVΔG-CHIKV (7×10^8 PFU) was stereotactically injected on the top of the tumor on both sides of the brain. Tumor (G) and control cerebellum (F) tissue samples were harvested and dissociated 2 and 10 days later and

used to inoculate cultures of Vero cells. VSVΔG-CHIKV infection of Vero cells was determined by immunostaining (scale bar, 0.5 mm) and percentages of infected cells are shown in the bar graph (H). Only tumor tissue generated infection on the underlying cells. ***$p < 0.001$.

Author Manuscript Author Manuscript Author Manuscript Author Manuscript

Author Manuscript Author Manuscript Author Manuscript Author Manuscript

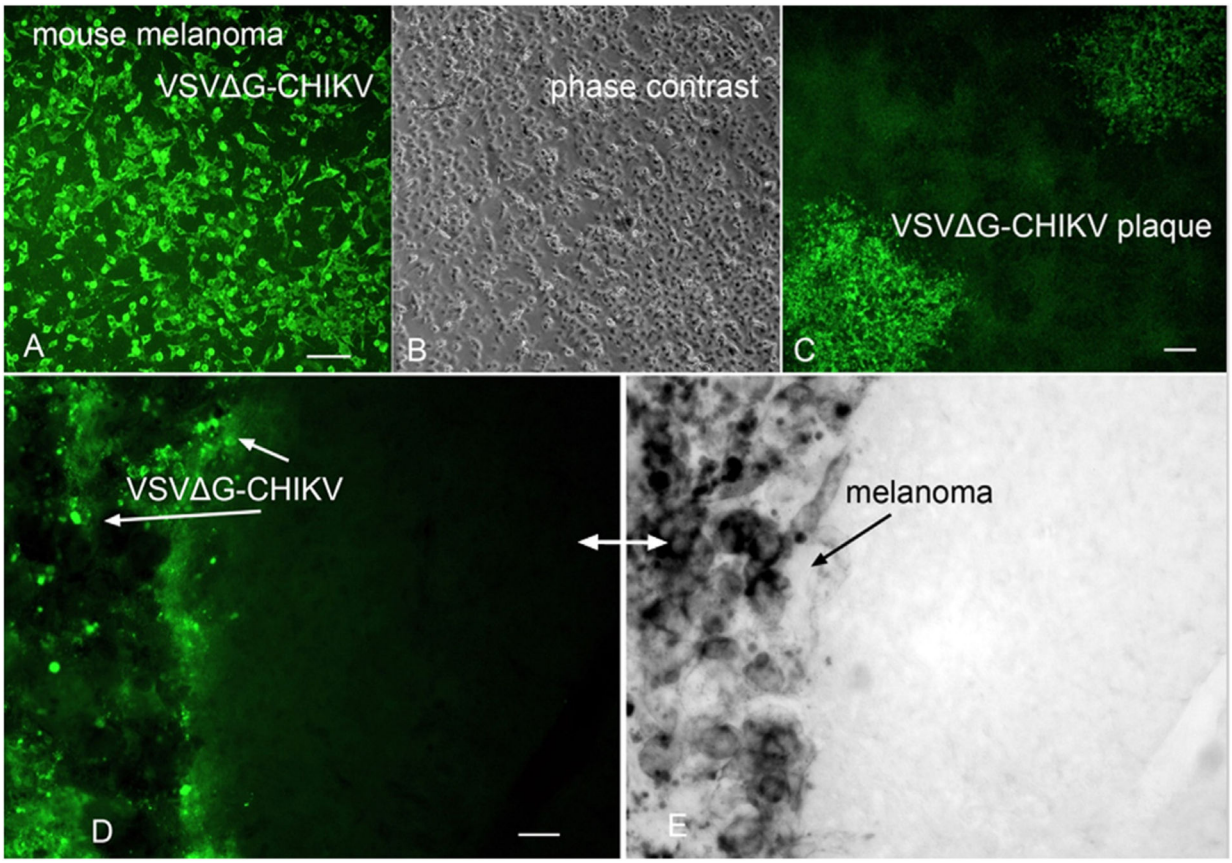

Fig. 12. VSVΔG-CHIKV targets mouse melanoma in immunocompetent mouse brain.

A. VSVΔG-CHIKV shows strong green infection of mouse B16F1 melanoma in vitro. Scale, 100 μm. **B.** Phase contrast image of melanoma cells from **A. C.** VSVΔG-CHIKV makes plaques (3 dpi) in cultured mouse melanoma. Scale 130 μm. **D.** Mouse melanoma B16F1 cells were implanted into the brain (n = 3); 7 days later VSVΔG-CHIKV was injected intracranially after the tumor expanded. At 4 dpi mice were euthanized. Immunostained green VSVΔG-CHIKV selectively infected the region where the dark (E) melanoma cells were found, with little infection of the normal brain on the right side of the micrograph. **D and E** show the same microscope field, with (D) showing virus immunofluorescence and (E) showing the dark melanoma on the left side of micrograph. The lighter color in (E) is normal brain tissue. Scale, 30 μm.

Author Manuscript Author Manuscript Author Manuscript Author Manuscript

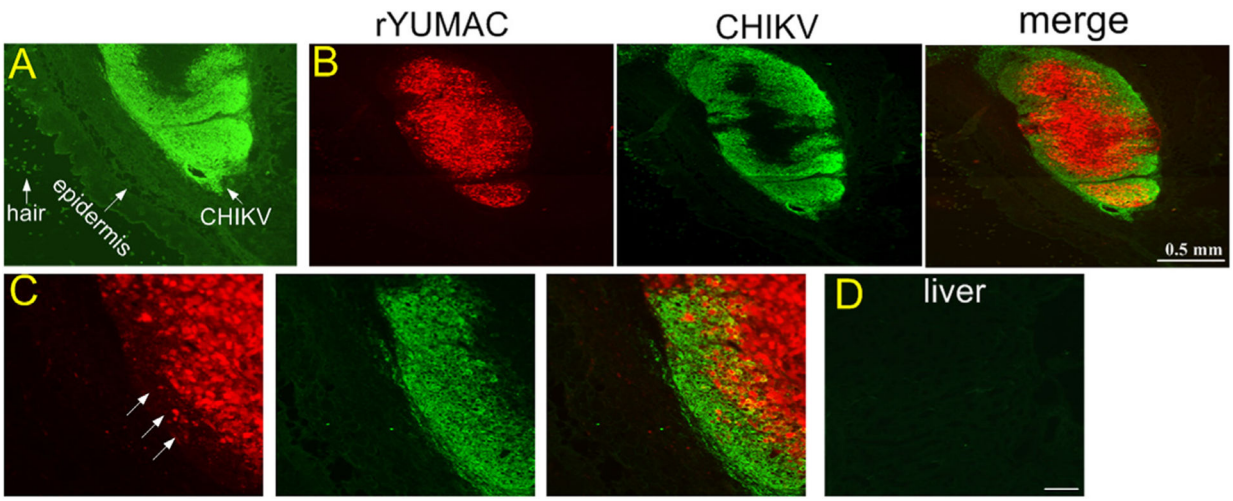

Fig. 13. Intravenous VSVΔG-CHIKV targets melanoma, but shows little infection of normal tissue.

CB17 SCID mice (n = 5) received subcutaneous injection of human rYUMAC melanoma cells (1×10^6 cells) expressing RFP. 11 days later, tail vain (i.v) injected 100 μl (8×10^8 PFU) of VSVΔG-CHIKV. Skin, brain, liver, spleen, lung, colon, bladder, kidney, heart, stomach and testis were harvested 4 days later. **A.** VSVΔG-CHIKV was found only in one location, identified as the implanted melanoma. **B.** Only the red YUMAC melanoma was infected, as shown by the red tumor and colocalization of the green immunostained virus. **C.** Higher magnification of (B). Arrows show a few remaining red cells as the virus appears to be moving toward the center of the tumor, and beginning to eliminate tumor cells at the periphery. **D.** No virus was detectable in normal tissue, as shown here in an immunostained section from liver. Scale bar, 0.5 mm (B) and 50 μm (D).